

The $\gamma\gamma \rightarrow ZZ$ process and the search for virtual SUSY effects at a $\gamma\gamma$ Collider.[†]

G.J. Gounaris^a, J. Layssac^b, P.I. Porfyriadis^a and F.M. Renard^b

^aDepartment of Theoretical Physics, Aristotle University of Thessaloniki,
Gr-54006, Thessaloniki, Greece.

^bPhysique Mathématique et Théorique, UMR 5825
Université Montpellier II, F-34095 Montpellier Cedex 5.

Abstract

We study the helicity amplitudes of the process $\gamma\gamma \rightarrow ZZ$ in the Standard Model at high energy. These amplitudes receive contributions from the W and charged quark and lepton loops, analogous to those encountered in the $\gamma\gamma \rightarrow \gamma\gamma$, γZ cases studied before. But $\gamma\gamma \rightarrow ZZ$ also receives contributions from the Higgs s-channel poles involving the effective Higgs- $\gamma\gamma$ vertex. At energies $\gtrsim 300\text{GeV}$, the amplitudes in all three processes are mainly helicity-conserving and almost purely imaginary; which renders them a very useful tool in searching for New Physics. As an example, a SUSY case is studied, and the signatures due to the virtual effects induced by a chargino-, charged slepton- or a lightest stop-loop in $\gamma\gamma \rightarrow ZZ$, are explored. These signatures, combined with the analogous ones in $\gamma\gamma \rightarrow \gamma\gamma$ and $\gamma\gamma \rightarrow \gamma Z$, should help identifying the nature of possible New Physics particles.

[†] Partially supported by the NATO grant CRG 971470 and by the Greek government grant PENED/95 K.A. 1795.

1 Introduction

In the previous papers [1, 2, 3] we have presented a thorough study of the processes $\gamma\gamma \rightarrow \gamma\gamma$ and $\gamma\gamma \rightarrow \gamma Z$ in the Standard (SM) and SUSY models. These processes do not appear at tree level, and first arise at 1-loop order. In the Standard Model (SM) at energies above 250 GeV, their most striking property is that they are strongly dominated by the two independent helicity amplitudes $F_{++++}(\hat{s}, \hat{t}, \hat{u})$ and $F_{+--+}(\hat{s}, \hat{t}, \hat{u}) = F_{+--+}(\hat{s}, \hat{u}, \hat{t})$, which moreover turn out to be largely imaginary; the effect being more pronounced at the smaller scattering angles. At such energies all the other helicity amplitudes are extremely small. This remarkable property is due to the fact that the real Sudakov-type log-squared terms contributed by the various 1-loop diagrams, cancel out for all physical amplitudes. As a result, the most important remaining contribution at high energy and fixed scattering angle, is due to the single-log, predominantly imaginary terms, contributed by the W -loop diagrams. These terms only affect the helicity conserving amplitudes. All other amplitudes receive comparable contributions from both the W and fermion loops, and turn out to be very small in SM. Since a similar property is naturally expected also for the process $\gamma\gamma \rightarrow ZZ$ at sufficient energies, we intend here to present its study.

The processes ($\gamma\gamma \rightarrow \gamma\gamma$, γZ , ZZ), could be measured at the future e^+e^- Linear Colliders (LC) [4], when operated as a $\gamma\gamma$ Collider ($LC_{\gamma\gamma}$) through backscattering of laser beams [5, 6]. In such a case the $\gamma\gamma$ c.m. energy could be as high as 80% of the initial e^+e^- c.m. energy, while an annual luminosity of $\bar{L}_{\gamma\gamma} \simeq 0.2\bar{L}_{ee} \simeq 100 fb^{-1}$ would be reasonably expected [6]. Polarized $\gamma\gamma$ beams can also be obtained using initially polarized electron beams and lasers.

The aforementioned simplicity of the SM amplitudes for the three processes ($\gamma\gamma \rightarrow \gamma\gamma$, γZ , ZZ), may someday render them a very useful in the search for New Physics (NP) [2]; particularly for NP characterized by appreciable imaginary contributions to the helicity conserving amplitudes [2]. Such effects could involve *e.g.* amplitudes containing CP violating phases; or even effects due to the possible existence of additional large space-dimensions, inducing contributions from strings of graviton- or Z - or γ -Kaluza-Klein states with, maybe, appreciable width-generated imaginary parts [7, 8].

As an example of such an NP search, we studied previously the effects induced by the various SUSY particle loops contributing to $\gamma\gamma \rightarrow \gamma\gamma$, γZ [1, 2, 3]. In these studies we concentrated on the idea that there is no CP-violating phase in the SUSY parameter space¹; so that energies above the threshold for the SUSY particle production are needed, for appreciable imaginary contributions to occur. Of course, at such energies, the SUSY particles will be also directly produced and studied with much higher statistics. Nevertheless, the experimental study of their virtual contribution to the three processes $\gamma\gamma \rightarrow \gamma\gamma$, γZ , ZZ , should provide independent information, which will help to identify their nature. Particularly because such virtual SUSY effects should in general be less sensitive to the soft symmetry breaking parameters, than the direct production ones.

As already indicated, in the present paper we complete our previous analysis of $\gamma\gamma \rightarrow \gamma\gamma$, γZ , by also studying the $\gamma\gamma \rightarrow ZZ$ amplitudes in the standard and SUSY models.

¹An investigation of the effects of such phases we intend to present in the future.

The distinctive feature of this later process (as opposed to the previous ones), is that it also receives contributions from the Higgs s-channel pole diagrams², which increase the sensitivity to the lightest stop, making it measurable. Of course $\gamma\gamma \rightarrow ZZ$ has also been studied before in SM [9, 10, 11], but explicit expressions for the for the W -loop contribution to the SM amplitudes have only by given by [9]. We have reproduced the results of these authors³ in Appendix A, choosing a different way of presentation though.

More explicitly, the expressions for the W [9] and fermion loop [12] contributions to the helicity amplitudes are given in Appendix A. In addition, we also give the 1-loop contribution induced by a single charged scalar particle. In Appendix B simple asymptotic expressions for the SM helicity amplitudes are given, which elucidate their physical properties at high energies.

In Sec.2 we discuss the main properties of the exact expressions for the W , fermion or scalar particle 1-loop contributions. This allows us to study the helicity amplitudes in SM, and to predict possible contributions due to new fermion or scalar particle loops. As an example we present the contributions to these amplitudes due to a gaugino- or higgsino-like chargino, an L- or R-slepton, or a lightest stop-loop. In all applications we assume no CP-violating phases in the soft SUSY breaking parameters, and work in the so called decoupling regime, where the CP-odd neutral Higgs particle is taken very heavy; $m_A^0 \gg m_Z$. Since the asymptotic expressions for the SM helicity amplitudes, derived in Appendix B, may be useful for quick calculations; we also offer in Sec. 2 a discussion of their region of validity.

In Sec. 3, we study the corresponding $\gamma\gamma \rightarrow ZZ$ cross sections for various polarizations of the incoming photons. We identify the sensitivity of these cross sections to various SUSY effects and we discuss their observability. Finally, in Sec. 4, we summarize the results and give our general conclusions for all three processes $\gamma\gamma \rightarrow \gamma\gamma$, γZ , ZZ .

2 An overall view of the $\gamma\gamma \rightarrow ZZ$ amplitudes.

The invariant helicity amplitudes $F_{\lambda_1\lambda_2\lambda_3\lambda_4}(\beta_Z, \hat{t}, \hat{u})$ for the process $\gamma\gamma \rightarrow ZZ$, with λ_j denoting the helicities of the incoming and outgoing particles, are given in Appendix A. As observed in [12, 9], the properties of the helicity polarization vectors suggest to describe the energy-dependence of these amplitudes in terms of the dimensionless variable β_Z related to the usual \hat{s} through $\hat{s} = 4m_Z^2/(1 - \beta_Z^2)$. In the ZZ -rest frame, β_Z describes the velocity of each Z , provided it is chosen to be positive. According to the discussion in Appendix A, the constraint (A.9), together with (A.6-A.7) and (A.10), arising from Bose symmetry and parity invariance respectively, reduce the number of independent helicity amplitudes to just eight. As in (A.11) of Appendix A, these are taken to be

$$\begin{aligned}
 & F_{++++}(\beta_Z, \hat{t}, \hat{u}), \quad F_{+---}(\beta_Z, \hat{t}, \hat{u}), \quad F_{+-++}(\beta_Z, \hat{t}, \hat{u}), \quad F_{-+00}(\beta_Z, \hat{t}, \hat{u}), \\
 & F_{++00}(\beta_Z, \hat{t}, \hat{u}), \quad F_{++0+}(\beta_Z, \hat{t}, \hat{u}), \quad F_{+-+0}(\beta_Z, \hat{t}, \hat{u}), \quad F_{+--+}(\beta_Z, \hat{t}, \hat{u}). \quad (1)
 \end{aligned}$$

²note that in $\gamma\gamma \rightarrow \gamma\gamma, \gamma Z$, the Higgs resonance contribution is only absent at one-loop order, while it contributes from two loops onwards.

³Apart from a minor misprint in the small F_{+-+0} amplitude, to be mentioned below.

As explained in Appendix A, the relations (A.12, A.13) implied from (A.9), determine through the ($\beta_Z \rightarrow -\beta_Z$) substitution, the two helicity amplitudes

$$F_{++--}(\beta_Z, \hat{t}, \hat{u}) = F_{++++}(-\beta_Z, \hat{t}, \hat{u}) \quad , \quad (2)$$

$$F_{++-0}(\beta_Z, \hat{t}, \hat{u}) = F_{+++0}(-\beta_Z, \hat{t}, \hat{u}) \quad , \quad (3)$$

while all the rest are obtained from the aforementioned ten, through helicity changes or ($\hat{t} \leftrightarrow \hat{u}$) interchanges.

In Appendix A, we reproduce the W and charged fermion contributions of [9, 12] to the eight basic amplitudes in (1); while in (A.32, A.33) we also give the contributions due to a loop realized by scalar particle carrying a definite weak isospin and charge. All results are given in terms of the standard 1-loop functions B_0 , C_0 and D_0 , first introduced in [13].

Explicit asymptotic expressions for these functions, as well as for the corresponding W , fermion and scalar loop contributions to the helicity amplitudes, are given in Appendix B. On the basis of them we conclude that in $\gamma\gamma \rightarrow ZZ$, (as well as in the process $\gamma\gamma \rightarrow \gamma\gamma$, γZ studied before), the Sudakov-type real log-squared terms always cancel out at high energies and fixed scattering angle. The dominant contributions then arise from logarithmically increasing imaginary terms generated by the W loop. It turns out that such terms exist only for the two helicity conserving amplitudes $F_{++++}(\beta_Z, \hat{t}, \hat{u})$ and $F_{+--+}(\beta_Z, \hat{t}, \hat{u}) = F_{+--+}(\beta_Z, \hat{u}, \hat{t})$; which are therefore the most important ones at high energies. These dominant amplitudes are largely imaginary and increase with energy, while all the rest tend asymptotically to quite negligible constants.

These results can be seen in Fig.1a,b, where the largest among the ten amplitudes in (1, 2, 3) are shown, using the exact 1-loop functions, at the c.m. scattering angles $\vartheta^* = 30^0$ and $\vartheta^* = 90^0$. It is shown in these figures that indeed at sufficient energies, the real parts of $F_{\pm\pm\pm\pm}(\beta_Z, \hat{t}, \hat{u})$ and $F_{\pm\mp\mp\pm}(\beta_Z, \hat{t}, \hat{u}) = F_{\pm\mp\mp\pm}(\beta_Z, \hat{u}, \hat{t})$ are always much smaller than the corresponding imaginary parts. The effect becomes less pronounced though, as the scattering angle increases.

We have also checked that for $\sqrt{\hat{s}} \gtrsim 300 \text{ GeV}$, the W -loop contribution completely dominates the large imaginary parts of the helicity conserving amplitudes; while the fermion and Higgs contributions are very small there. For the real parts of these amplitudes though, as well for the other (small) helicity amplitudes, the W contributions are at the same level as the other ones in SM; their sum being always very small. Similar results have also been observed for the $\gamma\gamma \rightarrow \gamma\gamma$ [2] and $\gamma\gamma \rightarrow \gamma Z$ [3] cases; but in these cases the asymptotic region starts already at $\sim 250 \text{ GeV}$.

To assess the quality of the SM asymptotic expressions given in Appendix B, we have compared them to the exact 1-loop results for the ten $\gamma\gamma \rightarrow ZZ$ amplitudes in (1, 2, 3). We find that at $\sqrt{\hat{s}} \simeq 1 \text{ TeV}$, the differences between the imaginary parts of the asymptotic and exact 1-loop results, are at the 10% level or smaller. At higher energies the agreement improves of course, reaching the level of the fourth significant digit at $\sim 10 \text{ TeV}$. For the other amplitudes though, almost complete cancellations among the various terms occur, particularly for $\hat{s} \gtrsim 1 \text{ TeV}^2$; leading to the conclusion, (common for both the asymptotic and the exact 1-loop expressions), that they are indeed negligible.

We next turn to the possible SUSY contributions to the various amplitudes. As such we study contributions from a chargino or a sfermion loop, either in diagrams with four external legs, or in Higgs-pole diagrams involving a Higgs- $\gamma\gamma$ vertex.

The chargino contribution.

The contribution from the lightest positively charged chargino $\tilde{\chi}_1^+$ is obtained from the effective interaction (A.52) by using [14, 15]

$$g_{v\tilde{\chi}_1}^Z = \frac{1}{2c_W s_W} \left\{ \frac{3}{2} - 2s_W^2 + \frac{1}{4}[\cos(2\phi_L) + \cos(2\phi_R)] \right\}, \quad (4)$$

$$g_{a\tilde{\chi}_1}^Z = \frac{1}{8c_W s_W} [\cos(2\phi_R) - \cos(2\phi_L)], \quad (5)$$

with

$$\begin{aligned} \cos(2\phi_L) &= -\frac{M_2^2 - \mu^2 - 2m_W^2 \cos(2\beta)}{\sqrt{(M_2^2 + \mu^2 + 2m_W^2)^2 - 4[M_2\mu - m_W^2 \sin(2\beta)]^2}}, \\ \cos(2\phi_R) &= -\frac{M_2^2 - \mu^2 + 2m_W^2 \cos(2\beta)}{\sqrt{(M_2^2 + \mu^2 + 2m_W^2)^2 - 4[M_2\mu - m_W^2 \sin(2\beta)]^2}}, \end{aligned} \quad (6)$$

and

$$M_{\tilde{\chi}_1^+}^2 = \frac{1}{2} \left\{ M_2^2 + \mu^2 + 2m_W^2 - \sqrt{(M_2^2 + \mu^2 + 2m_W^2)^2 - 4[M_2\mu - m_W^2 \sin(2\beta)]^2} \right\}, \quad (7)$$

where M_2 and μ are taken real, and β is the usual SUSY parameter. These formulae should be combined with (A.53, A.55 -A.71) in Appendix A, in order to calculate the chargino loop contribution to the four-leg diagrams.

In SUSY, the Higgs-pole contribution, due to the lightest chargino $\tilde{\chi}_1^+$ loop affecting the Higgs- $\gamma\gamma$ vertex, may in general involve any of the two CP-even neutral Higgs states h^0 or H^0 . Since we will be working below in the so called decoupling regime, where $m_A \sim m_{H^0} \sim m_{H^\pm} \gg m_Z$, we only need the $h^0 ZZ$ and $h^0 \chi_1^+ \chi_1^-$ interaction lagrangian [14]

$$\begin{aligned} \mathcal{L}_{h^0 ZZ, h^0 \chi_1^+ \chi_1^-} &= \frac{gm_Z}{2c_W} \sin(\beta - \alpha) h^0 Z_\mu Z^\mu \\ &- \frac{g}{\sqrt{2}} [-\sin \alpha \cos \phi_R \sin \phi_L + \cos \alpha \cos \phi_L \sin \phi_R] h^0 \tilde{\chi}_1^+ \tilde{\chi}_1^-. \end{aligned} \quad (8)$$

Comparing this with (A.26) and working in the decoupling SUSY regime where $\alpha = \beta - \pi/2$, we write the lightest chargino contribution to the curly brackets in (A.25) as

$$\mathcal{H}_{\tilde{\chi}_1^+}(\tau_{\tilde{\chi}_1^+}) = \frac{\sqrt{2}m_W}{m_{\tilde{\chi}_1^+}} [\cos \beta \cos \phi_R \sin \phi_L + \sin \beta \cos \phi_L \sin \phi_R] F_{1/2}(\tau_{\tilde{\chi}_1^+}), \quad (9)$$

where

$$\tau_{\tilde{\chi}_1^+} \equiv \frac{4m_{\tilde{\chi}_1^+}^2}{\hat{s}}, \quad (10)$$

and (A.29, A.31) should be used.

Using the relations (4-10), together with the results (A.25, A.53, A.55-A.71) of Appendix A, and the exact calculation of the 1-loop functions provided by [16], we present in Fig.2 the results for two almost "extreme" situations corresponding to a light chargino of mass $M_{\tilde{\chi}_1^+} \simeq 95 \text{ GeV}$, with $\tan\beta = 2$ and $\mu < 0$. In the first case the chargino nature is taken gaugino-like, by choosing (see Fig.2a,b)

$$\begin{aligned} M_2 &= 81 \text{ GeV} \quad , \quad \mu = -215 \text{ GeV} \quad , \\ g_{v\tilde{\chi}_1}^Z &= 1.72 \quad , \quad g_{a\tilde{\chi}_1}^Z = 0.102 \quad ; \end{aligned} \quad (11)$$

while in the second case it is taken "higgsino-like" by choosing (see Fig.2c,d)

$$\begin{aligned} M_2 &= 215 \text{ GeV} \quad , \quad \mu = -81 \text{ GeV} \\ g_{v\tilde{\chi}_1}^Z &= 0.76 \quad , \quad g_{a\tilde{\chi}_1}^Z = 0.113 \quad . \end{aligned} \quad (12)$$

The conclusion from Fig.2 is that $\gamma\gamma \rightarrow ZZ$ is much more sensitive to a gaugino-like chargino, than to a higgsino-like. This fact was also observed in the $\gamma\gamma \rightarrow \gamma Z$ case; while $\gamma\gamma \rightarrow \gamma\gamma$ is of course equally sensitive to both. The Higgs-pole contribution turns out to be quite small in the chargino case; so that the main effect arises from the chargino loop in the four-external-leg diagrams. Similar results, would also be obtained if the gaugino-like state would correspond to a $\mu > 0$ solution, like *e.g.* $M_{\tilde{\chi}_1^+} \simeq 96 \text{ GeV}$, $\tan\beta = 2.5$, $M_2 = 120 \text{ GeV}$ and $\mu = 300 \text{ GeV}$ [17].

The contributions from a slepton or the lightest stop \tilde{t}_1

As in the chargino case, we consider the decoupling limit $\alpha = \beta - \pi/2$ for the charged slepton and the lightest stop contributions. Then, the mass-terms and the $h^0 \tilde{e}_{L(R)}^* \tilde{e}_{L(R)}$ and $h^0 \tilde{t}_1^* \tilde{t}_1$ interaction Lagrangian are given by [14, 18]

$$\begin{aligned} \mathcal{L}_{h^0 \tilde{f} \tilde{f}} &= - (\tilde{t}_L^* \quad \tilde{t}_R^*) \begin{pmatrix} M_{\tilde{t}L}^2 + m_t^2 & m_t \tilde{A}_t \\ m_t \tilde{A}_t & M_{\tilde{t}R}^2 + m_t^2 \end{pmatrix} \begin{pmatrix} \tilde{t}_L \\ \tilde{t}_R \end{pmatrix} - M_{\tilde{e}L}^2 \tilde{e}_L^* \tilde{e}_L - M_{\tilde{e}R}^2 \tilde{e}_R^* \tilde{e}_R \\ &\quad - \frac{gm_Z^2}{m_W} \cos(2\beta) h^0 \left[\left(\frac{1}{2} - \frac{2}{3} s_W^2 \right) \tilde{t}_L^* \tilde{t}_L + \frac{2s_W^2}{3} \tilde{t}_R^* \tilde{t}_R + \left(-\frac{1}{2} + s_W^2 \right) \tilde{e}_L^* \tilde{e}_L - s_W^2 \tilde{e}_R^* \tilde{e}_R \right] \\ &\quad - \frac{gm_t \tilde{A}_t}{2m_W} h^0 (\tilde{t}_L^* \tilde{t}_R + \tilde{t}_R^* \tilde{t}_L) - \frac{gm_t^2}{m_W} h^0 (\tilde{t}_L^* \tilde{t}_L + \tilde{t}_R^* \tilde{t}_R) \quad , \end{aligned} \quad (13)$$

where

$$\tilde{A}_t = A_t - \mu \cot(\beta) \quad , \quad (14)$$

and $M_{\tilde{t}L}$, $M_{\tilde{t}R}$, $M_{\tilde{e}L}$, $M_{\tilde{e}R}$, A_t are the usual soft breaking parameters in the stop and slepton sector [14, 18]. Eqs. (13, 14) determine the sfermion Higgs-pole contributions and possible mixing; while the loop contributions due to a scalar particle with definite weak isospin and charge, are given by (A.32-A.41).

We first discuss the charged slepton case for which there is no appreciable mixing, so that we are lead to a pure *e.g.* L- or R-selectron circulating along the loop; compare (13).

Taking a common mass $M_{\tilde{e}} = M_{\tilde{e}_L} = M_{\tilde{e}_R} = 0.1 \text{ TeV}$, for both $(\tilde{e}_L, \tilde{e}_R)$ in (13); we get for a selectron loop with definite isospin and charge

$$g_{\tilde{e}}^Z = \frac{1}{c_W s_W} [t_3^{\tilde{e}} - Q_{\tilde{e}} s_W^2] \quad , \quad (15)$$

to be used in (A.32 - A.41) in Appendix A, with $Q_{\tilde{e}_L} = Q_{\tilde{e}_R} = -1$, $t_3^{\tilde{e}_L} = -\frac{1}{2}$ and $t_3^{\tilde{e}_R} = 0$; compare (A.33).

For an L-selectron this leads to $g_{\tilde{e}_L}^Z = -0.65$, while the Higgs-pole contribution is obtained by comparing (13, A.26) to be

$$\mathcal{H}_{\tilde{e}_L}(\tau_{\tilde{e}}) = \frac{m_Z^2}{M_{\tilde{e}}^2} \cos(2\beta) \left(-\frac{1}{2} + s_W^2\right) F_0(\tau_{\tilde{e}}) \quad , \quad (16)$$

where

$$\tau_{\tilde{e}} = \frac{4M_{\tilde{e}}^2}{\hat{s}} \quad . \quad (17)$$

Correspondingly, for an R-selectron, we have $g_{\tilde{e}_R}^Z = +0.54$, while the Higgs-pole contribution is determined by

$$\mathcal{H}_{\tilde{e}_R}(\tau_{\tilde{e}}) = \frac{m_Z^2}{M_{\tilde{e}}^2} \cos(2\beta) (-s_W^2) F_0(\tau_{\tilde{e}}) \quad . \quad (18)$$

Substituting in (A.25, A.32), we find that the R- and L-selectrons give very similar contributions to the $\gamma\gamma \rightarrow ZZ$ amplitudes; which is confirmed by the results in Fig.3a-d, derived using the exact 1-loop functions in (A.34 - A.41). We recall that the R- and L-selectrons contribute in the same way also in the $\gamma\gamma \rightarrow \gamma\gamma$ amplitudes, while their contributions to $\gamma\gamma \rightarrow \gamma Z$ have opposite signs [1, 3]. It seems that $\gamma\gamma \rightarrow \gamma\gamma$ is somewhat more sensitive to slepton contributions, than the other two processes $\gamma\gamma \rightarrow \gamma Z$, ZZ . It is also found that the slepton contributions to F_{++++} and F_{++00} , due to the Higgs-pole or the four-leg loop diagrams, are comparable.

We next turn to the contribution from the lightest stop, denoted as \tilde{t}_1 , which is obtained by taking into account the mixing implied by (13). For real $M_{\tilde{t}_L}$, $M_{\tilde{t}_R}$ and \tilde{A}_t , this leads to

$$\begin{pmatrix} \tilde{t}_L \\ \tilde{t}_R \end{pmatrix} = \begin{pmatrix} \cos \theta_t & -\sin \theta_t \\ \sin \theta_t & \cos \theta_t \end{pmatrix} \begin{pmatrix} \tilde{t}_1 \\ \tilde{t}_2 \end{pmatrix} \quad (19)$$

$$m_{\tilde{t}_1, \tilde{t}_2}^2 = \frac{1}{2} \left\{ M_{\tilde{t}_L}^2 + M_{\tilde{t}_R}^2 + 2m_t^2 \mp \sqrt{(M_{\tilde{t}_L}^2 - M_{\tilde{t}_R}^2)^2 + 4m_t^2 \tilde{A}_t^2} \right\} \quad , \quad (20)$$

$$\sin(2\theta_t) = \frac{2m_t \tilde{A}_t}{m_{\tilde{t}_1}^2 - m_{\tilde{t}_2}^2} \quad , \quad \cos(2\theta_t) = \frac{M_{\tilde{t}_L}^2 - M_{\tilde{t}_R}^2}{m_{\tilde{t}_1}^2 - m_{\tilde{t}_2}^2} \quad . \quad (21)$$

Then, the Z -stop coupling to be used in conjunction with (A.32) is

$$g_{\tilde{t}_1}^Z = \frac{1}{2c_W s_W} \left(\cos^2 \theta_t - \frac{4}{3} s_W^2 \right) \quad , \quad (22)$$

while (13, A.26, A.25) determine the \tilde{t}_1 Higgs-pole contribution by

$$\mathcal{H}_{\tilde{t}_1}(\tau_{\tilde{t}_1}) = \frac{3}{m_{\tilde{t}_1}^2} \left\{ m_Z^2 \cos(2\beta) \left[\frac{\cos^2 \theta_t}{2} - \frac{2s_W^2}{3} \cos(2\theta_t) \right] + \frac{m_t \tilde{A}_t}{2} \sin(2\theta_t) + m_t^2 \right\} F_0(\tau_{\tilde{t}_1}), \quad (23)$$

where

$$\tau_{\tilde{t}_1} = \frac{4m_{\tilde{t}_1}^2}{\hat{s}}, \quad (24)$$

and the factor three for colour multiplicity has been included.

An example of a lightest stop contribution to the $\gamma\gamma \rightarrow ZZ$ amplitudes is given in Fig.4, corresponding to the assumption that $M_{\tilde{t}_L} = M_{\tilde{t}_R}$ are chosen so that $m_{\tilde{t}_1} = 100 \text{ GeV}$, and $\tilde{A}_t = 1 \text{ TeV}$. In such a case we get $\theta_t = 3\pi/4$. As shown in Fig.4, the \tilde{t}_1 contributions to the amplitudes, are almost independent of ϑ^* ; which simply indicates the dominance of the Higgs-pole contribution.

A comparison of Fig.2a-d, Fig.3a-d and Fig.4a,b indicates that the most promising effects are generated either by a gaugino-like chargino, or from the lightest stop \tilde{t}_1 . Most of the \tilde{t}_1 effect arises from the Higgs-pole contribution to the amplitudes. This explains why the stop effect is much smaller in the $\gamma\gamma \rightarrow \gamma\gamma, \gamma Z$ cases [1, 3], where this last contribution is absent.

3 The $\gamma\gamma \rightarrow ZZ$ Cross sections

We next explore the possibility to use polarized or unpolarized $\gamma\gamma$ collisions in an $LC_{\gamma\gamma}$ Collider [2]. As in the $\gamma\gamma \rightarrow \gamma\gamma$ case [1], Bose statistics and Parity invariance leads to

$$\begin{aligned} \frac{d\sigma}{d\tau d \cos \vartheta^*} &= \frac{d\bar{L}_{\gamma\gamma}}{d\tau} \left\{ \frac{d\bar{\sigma}_0}{d \cos \vartheta^*} + \langle \xi_2 \xi_2' \rangle \frac{d\bar{\sigma}_{22}}{d \cos \vartheta^*} + [\langle \xi_3 \rangle \cos 2\phi + \langle \xi_3' \rangle \cos 2\phi'] \frac{d\bar{\sigma}_3}{d \cos \vartheta^*} \right. \\ &\quad \left. + \langle \xi_3 \xi_3' \rangle \left[\frac{d\bar{\sigma}_{33}}{d \cos \vartheta^*} \cos 2(\phi + \phi') + \frac{d\bar{\sigma}'_{33}}{d \cos \vartheta^*} \cos 2(\phi - \phi') \right] \right. \\ &\quad \left. + [\langle \xi_2 \xi_3' \rangle \sin 2\phi' - \langle \xi_3 \xi_2' \rangle \sin 2\phi] \frac{d\bar{\sigma}_{23}}{d \cos \vartheta^*} \right\}, \quad (25) \end{aligned}$$

where

$$\frac{d\bar{\sigma}_0(\gamma\gamma \rightarrow ZZ)}{d \cos \vartheta^*} = \left(\frac{\beta_Z}{128\pi\hat{s}} \right) \sum_{\lambda_3\lambda_4} [|F_{++\lambda_3\lambda_4}|^2 + |F_{+-\lambda_3\lambda_4}|^2], \quad (26)$$

$$\frac{d\bar{\sigma}_{22}(\gamma\gamma \rightarrow ZZ)}{d \cos \vartheta^*} = \left(\frac{\beta_Z}{128\pi\hat{s}} \right) \sum_{\lambda_3\lambda_4} [|F_{++\lambda_3\lambda_4}|^2 - |F_{+-\lambda_3\lambda_4}|^2], \quad (27)$$

$$\frac{d\bar{\sigma}_3(\gamma\gamma \rightarrow ZZ)}{d \cos \vartheta^*} = \left(\frac{-\beta_Z}{64\pi\hat{s}} \right) \sum_{\lambda_3\lambda_4} \text{Re}[F_{++\lambda_3\lambda_4} F_{-+\lambda_3\lambda_4}^*], \quad (28)$$

$$\frac{d\bar{\sigma}_{33}(\gamma\gamma \rightarrow ZZ)}{d \cos \vartheta^*} = \left(\frac{\beta_Z}{128\pi\hat{s}} \right) \sum_{\lambda_3\lambda_4} \text{Re}[F_{+-\lambda_3\lambda_4} F_{-+\lambda_3\lambda_4}^*], \quad (29)$$

$$\frac{d\bar{\sigma}'_{33}(\gamma\gamma \rightarrow ZZ)}{d \cos \vartheta^*} = \left(\frac{\beta_Z}{128\pi\hat{s}} \right) \sum_{\lambda_3\lambda_4} \text{Re}[F_{++\lambda_3\lambda_4} F_{--\lambda_3\lambda_4}^*], \quad (30)$$

$$\frac{d\bar{\sigma}_{23}(\gamma\gamma \rightarrow ZZ)}{d \cos \vartheta^*} = \left(\frac{\beta_Z}{64\pi\hat{s}} \right) \sum_{\lambda_3\lambda_4} \text{Im}[F_{++\lambda_3\lambda_4} F_{+-\lambda_3\lambda_4}^*], \quad (31)$$

are expressed in terms of the amplitudes given in Appendix A. The quantity $d\bar{L}_{\gamma\gamma}/d\tau$ in (25), describes the photon-photon luminosity per unit e^-e^+ flux, in an LC operated in the $\gamma\gamma$ mode [5]. The Stokes parameters ξ_2, ξ_3 and the azimuthal angle ϕ in (25), determine the normalized most general helicity density matrix of one of the backscattered photons $\rho_{\lambda\lambda}^{BN}$, through the formalism described in Appendix B of [1]; compare Eq.(B4) of [1]. The corresponding parameters for the other backscattered photon are denoted by a prime. The numerical expectations for $d\bar{L}_{\gamma\gamma}/d\tau$, $\langle \xi_j \rangle$, $\langle \xi'_j \rangle$ and $\langle \xi_i \xi'_j \rangle$ are given in Appendix B and Fig.4 of [1].

In (26 - 31), β_Z is the Z velocity in the ZZ frame, while ϑ^* is the scattering angle, and $\tau \equiv s_{\gamma\gamma}/s_{ee}$. Because of Bose statistics, all $d\bar{\sigma}_j/d \cos \vartheta^*$ are forward-backward symmetric. Note that $d\bar{\sigma}_0/d \cos \vartheta^*$ is the unpolarized cross section. This is the only $\bar{\sigma}_j$ quantity which is positive definite.

The results for the differential cross sections $d\bar{\sigma}_j/d \cos \vartheta^*$, are given in Fig.5a-f at $\sqrt{\hat{s}} = 0.5 \text{ TeV}$; while the corresponding integrated cross sections in the range $30^\circ \leq \vartheta^* \leq 150^\circ$, appear as functions of $\sqrt{\hat{s}}$, in Fig.6a-f. In each case we give the standard model (SM) predictions; as well as the results expected for the cases of including the contributions from a single chargino or a single charged slepton or the \tilde{t}_1 . For each of these SUSY contributions, we use the same parameters as those appearing in the amplitudes presented in Fig.2-4.

When comparing the general structure of the differential cross sections in Fig.5a-f, with the corresponding results for $\gamma\gamma \rightarrow \gamma\gamma$ and γZ [1, 3], we remark the following. The general shape of $d\bar{\sigma}_0/d \cos \vartheta^*$ is roughly the same in all three cases. Exactly the opposite shape, with central a peak (at $\vartheta^* \simeq \pi/2$) and a dip in the forward and backward regions, is found for $d\bar{\sigma}_{22}/d \cos \vartheta^*$ in the $\gamma\gamma \rightarrow \gamma\gamma$ case; while for $\gamma\gamma \rightarrow \gamma Z$ we find something like a plateau in the central region; which develops to a central dip and two peaks at $\vartheta^* \simeq \pi/4, 3\pi/4$ for $\gamma\gamma \rightarrow ZZ$; compare Fig.6b of [3] and Fig.5b of this paper.

The other cross sections are much smaller. Paying attention only to the largest ones, we remark that $d\bar{\sigma}_{33}/d \cos \vartheta^*$ has a central-peak and a forward-backward dip structure for all processes; compare Fig.6e in [1] with Fig.5e here. On the other hand, $d\bar{\sigma}_3/d \cos \vartheta^*$ has a central plateau and forward and backward dips in $\gamma\gamma \rightarrow ZZ$; which become a central plateau accompanied with forward and backward peaks in $\gamma\gamma \rightarrow \gamma\gamma$; while in $\gamma\gamma \rightarrow \gamma Z$ it is not forward-backward symmetric; compare Fig.6d of [3] and Fig.5c.

Concerning the relative (NP versus SM) effects, the main difference between $\gamma\gamma \rightarrow ZZ$, and $(\gamma\gamma \rightarrow \gamma\gamma, \gamma Z)$, is that the former displays considerable sensitivity to the lightest stop \tilde{t}_1 , which is not shared by the other two. This is because the lightest stop contribution

is mainly generated by the Higgs-pole diagrams; which of course do not contribute to $\gamma\gamma \rightarrow \gamma\gamma$, γZ . Such \tilde{t}_1 effects are mostly visible in $d\bar{\sigma}_{22}/d\cos\vartheta^*$ and $d\bar{\sigma}_3/d\cos\vartheta^*$ shown in Fig.5b,c, and in $\bar{\sigma}_{22}$ in Fig6c.

With respect to the chargino signatures, the fact is that $\gamma\gamma \rightarrow ZZ$ and $\gamma\gamma \rightarrow \gamma Z$ are mainly sensitive to a gaugino-type chargino; while $\gamma\gamma \rightarrow \gamma\gamma$ is equally sensitive to both, the gaugino- as well as the higgsino-type charginos. Finally, very little sensitivity to charged sleptons is displayed by all three processes $\gamma\gamma \rightarrow \gamma\gamma$, γZ , ZZ .

To make the discussion of the observability of the various NP effects in the differential cross sections in (25) more quantitative, we should take into account the experimental aspects of the $\gamma\gamma$ collision realized through laser backscattering [5, 6]. We proceed along the same lines as for the analysis of the observable quantities for $\gamma\gamma \rightarrow \gamma Z$ in Section 3 of [3]. The differential cross sections for $\gamma\gamma \rightarrow ZZ$ in Fig.5a-f, are in almost all cases⁴ about a factor of 2 larger than the corresponding cross sections for $\gamma\gamma \rightarrow \gamma Z$ shown in Fig.6a-f of [3]. Of course, for estimating the number of the measurable ZZ -production events, some ZZ identification factor should be taken into account. A corresponding factor is apparently not needed in the γZ production case, since the photon provides a very good signature. Assuming that the useful modes for the ZZ identification are those where one Z decays leptonically (including the invisible neutrino mode), and the other hadronically, we get an identification factor of about 1/2; if only charged leptons are used for the leptonic modes this factor decreases to 20 percent. So finally, the useful ZZ rate is comparable to the γZ one. Thus, the statistical uncertainties in measuring the various ZZ cross sections are similar to those of the corresponding γZ ones appearing in [3]. Therefore, we expect that it should be possible to attain an absolute accuracy of about $0.3fb$ for $d\bar{\sigma}_0(\gamma\gamma \rightarrow ZZ)/d\cos\vartheta^*$ at large angles. Correspondingly, an absolute accuracy of about $(0.3 - 3)fb$, (depending on the flux optimization), should be realistic for the smaller quantities $d\bar{\sigma}_{22}/d\cos\vartheta^*$, $d\bar{\sigma}_3/d\cos\vartheta^*$ and $d\bar{\sigma}_{33}/d\cos\vartheta^*$ at large angles.

Therefore, the $\gamma\gamma \rightarrow ZZ$ sensitivity to a gaugino-type chargino of $\sim 100 GeV$, is similar and even more pronounced than the sensitivity of the $\gamma\gamma \rightarrow \gamma Z$ process; while the higgsino or slepton effects are more depressed in $\gamma\gamma \rightarrow ZZ$ [3]. The important feature of the ZZ production is its sensitivity to a \tilde{t}_1 contribution, which may be comparable to the gaugino or higgsino sensitivity, provided that sufficient transverse and longitudinal polarizations for the photon beams are available. We also note that in the present case we have explored this sensitivity only in the decoupling limit.

The illustrations given in the present paper are for a chargino, slepton, or a lightest stop \tilde{t}_1 in 100 GeV mass range. For higher masses, the relative merits of the $\gamma\gamma \rightarrow ZZ$, $\gamma\gamma \rightarrow \gamma Z$ and $\gamma\gamma \rightarrow \gamma\gamma$ processes⁵ remain about the same. These processes should be very helpful in identifying the nature of the various sparticles, up to masses of about 300 GeV.

⁴The exception applies only to the case of $d\bar{\sigma}_{23}/d\cos\vartheta^*$, which is very small in SM, anyway.

⁵ In [1] we gave some illustration for sparticles at 250 GeV in the $\gamma\gamma \rightarrow \gamma\gamma$ case.

4 Conclusions

In this paper we have studied the helicity amplitudes and observables for the process $\gamma\gamma \rightarrow ZZ$. Combining this with previous work in [1, 3, 19, 20, 21, 9], we get the complete set of all relevant formulae for calculating the helicity amplitudes of the three processes $\gamma\gamma \rightarrow \gamma\gamma$, γZ , ZZ in SM and SUSY.

The striking property of these three processes in SM above $\sim 300\text{GeV}$, is that they are strongly dominated by just the two helicity-conserving amplitudes $F_{++++}(\hat{s}, \hat{t}, \hat{u})$ and $F_{\pm\mp\pm\mp}(\hat{s}, \hat{t}, \hat{u}) = F_{\pm\mp\mp\pm}(\hat{s}, \hat{u}, \hat{t})$; which moreover are largely imaginary. This simple structure is solely generated by the W -loop, which at these energies, has exactly the same structure as the one expected from a Pomeron contribution. But the magnitude of this "weakly interacting" W -loop contribution is much larger than any reasonable expectation we might have for the "strongly interacting" Pomeron. If the $LC_{\gamma\gamma}$ Collider is ever realized, it will be amusing to check this!

Furthermore, the aforementioned simple properties of the SM amplitudes of the above processes, should make them a very efficient tool in searching for New Physics (NP) involving substantial imaginary amplitudes. As a first example here and in [1, 3] we studied the contributions from loops involving charginos or sleptons or the stop squark, in SUSY models with no CP violating phases beyond the SM ones. Thus, these first examples have been only applied to energies above the threshold for sparticle production.

Such measurements should be particularly useful when we would confront the question of identifying the nature of any possible SUSY candidate. If such a stage is ever reached, then these loop effects, being less (or at least differently depending) on the soft SUSY breaking parameters, would supply important information on the nature of such candidates. Particularly clear is the distinction between a gaugino-type chargino which should give an observable effect to all the three processes above; as opposed to \tilde{t}_1 contribution which should only be visible at $\gamma\gamma \rightarrow ZZ$; provided of course that these SUSY particles are not too heavy. Similarly, a higgsino type chargino with mass around 100 GeV, will only be visible at $\gamma\gamma \rightarrow \gamma\gamma$ [1].

The standard SUSY scenarios we have explored in the present and previous papers [2, 1, 3], certainly do not exhaust the possibilities to use $\gamma\gamma \rightarrow \gamma\gamma$, γZ , ZZ , in order to probe new physics. They should certainly exist many more, particularly related to complex phases, that the NP amplitudes might for some reason have [2]. Within the SUSY framework, the next thing of this type that comes to mind, is to explore the sensitivity to the CP violating phases affecting the soft SUSY breaking parameters. This should affect both chargino and stop contributions. Furthermore, in explorations of the SUSY parameter space away from the decoupling limit, contributions from the heavier CP-even H^0 -pole may also affect $\gamma\gamma \rightarrow ZZ$, providing useful information.

The overwhelming dominance of the imaginary parts of the two helicity conserving amplitudes in $\gamma\gamma \rightarrow \gamma\gamma$, γZ , ZZ at high energies in SM, is simply so strikingly exclusive, that it cannot stand without some useful consequences. This constitutes a strong motivation for the achievement of high energy polarized photon-photon collisions.

Appendix A: The $\gamma\gamma \rightarrow ZZ$ helicity amplitudes in the Standard and SUSY models.

The invariant helicity amplitudes for the process

$$\gamma(p_1, \lambda_1)\gamma(p_2, \lambda_2) \rightarrow Z(p_3, \lambda_3)Z(p_4, \lambda_4) \quad , \quad (\text{A.1})$$

are denoted as⁶ $F_{\lambda_1\lambda_2\lambda_3\lambda_4}(\beta_Z, \hat{t}, \hat{u})$, where the momenta and helicities of the incoming photons and outgoing Z 's are indicated in parentheses, and the definitions

$$\hat{s} = (p_1 + p_2)^2 = \frac{4m_Z^2}{1 - \beta_Z^2} \quad , \quad \hat{t} = (p_1 - p_3)^2 \quad , \quad \hat{u} = (p_1 - p_4)^2 \quad , \quad (\text{A.2})$$

$$\hat{s}_4 = \hat{s} - 4m_Z^2 \quad , \quad \hat{s}_2 = \hat{s} - 2m_Z^2 \quad , \quad \hat{t}_1 = \hat{t} - m_Z^2 \quad , \quad \hat{u}_1 = \hat{u} - m_Z^2 \quad (\text{A.3})$$

are used. The parameter β_Z in (A.2) coincides with the Z -velocity in the ZZ c.m. frame, and it is convenient to be used instead of \hat{s} . Denoting by ϑ^* the c.m. scattering angle of $\gamma\gamma \rightarrow ZZ$, we also note

$$\hat{t} = m_Z^2 - \frac{\hat{s}}{2}(1 - \beta_Z \cos \vartheta^*) \quad , \quad \hat{u} = m_Z^2 - \frac{\hat{s}}{2}(1 + \beta_Z \cos \vartheta^*) \quad , \quad (\text{A.4})$$

$$Y = \hat{t}\hat{u} - m_Z^4 = \frac{s^2\beta_Z^2}{4}\sin^2 \vartheta^* = \hat{s}p_{TZ}^2 \quad , \quad \Delta = \sqrt{\frac{\hat{s}m_Z^2}{2Y}} \quad , \quad (\text{A.5})$$

where p_{TZ} is the Z transverse momentum.

Bose statistics, combined with the Jacob-Wick (JW) phase conventions⁷ for the helicity wavefunction of the so called second particle, demands

$$F_{\lambda_1\lambda_2\lambda_3\lambda_4}(\beta_Z, \hat{t}, \hat{u}) = F_{\lambda_2\lambda_1\lambda_4\lambda_3}(\beta_Z, \hat{t}, \hat{u})(-1)^{\lambda_3 - \lambda_4} \quad , \quad (\text{A.6})$$

$$F_{\lambda_1\lambda_2\lambda_3\lambda_4}(\beta_Z, \hat{t}, \hat{u}) = F_{\lambda_2\lambda_1\lambda_3\lambda_4}(\beta_Z, \hat{u}, \hat{t})(-1)^{\lambda_3 - \lambda_4} \quad , \quad (\text{A.7})$$

$$F_{\lambda_1\lambda_2\lambda_3\lambda_4}(\beta_Z, \hat{t}, \hat{u}) = F_{\lambda_1\lambda_2\lambda_4\lambda_3}(\beta_Z, \hat{u}, \hat{t}) \quad ; \quad (\text{A.8})$$

while the standard form of the Z polarization vectors implies the constraint

$$F_{\lambda_1\lambda_2\lambda_3\lambda_4}(\beta_Z, \hat{t}, \hat{u}) = F_{\lambda_1\lambda_2, -\lambda_3, -\lambda_4}(-\beta_Z, \hat{t}, \hat{u})(-1)^{\lambda_3 - \lambda_4} \quad . \quad (\text{A.9})$$

Finally, parity invariance implies

$$F_{\lambda_1\lambda_2\lambda_3\lambda_4}(\beta_Z, \hat{t}, \hat{u}) = F_{-\lambda_1, -\lambda_2, -\lambda_3, -\lambda_4}(\beta_Z, \hat{t}, \hat{u})(-1)^{\lambda_3 - \lambda_4} \quad . \quad (\text{A.10})$$

As a result, the 36 helicity amplitudes may be expressed in terms of just the eight independent ones

$$\begin{aligned} & F_{++++}(\beta_Z, \hat{t}, \hat{u}) \quad , \quad F_{++++}(\beta_Z, \hat{t}, \hat{u}) \quad , \quad F_{+--+}(\beta_Z, \hat{t}, \hat{u}) \quad , \quad F_{+-00}(\beta_Z, \hat{t}, \hat{u}) \quad , \\ & F_{++00}(\beta_Z, \hat{t}, \hat{u}) \quad , \quad F_{+++0}(\beta_Z, \hat{t}, \hat{u}) \quad , \quad F_{+-+0}(\beta_Z, \hat{t}, \hat{u}) \quad , \quad F_{+--+}(\beta_Z, \hat{t}, \hat{u}) \quad . \end{aligned} \quad (\text{A.11})$$

⁶Their sign is related to the sign of the S -matrix through $S_{\lambda_1\lambda_2\lambda_3\lambda_4} = 1 + i(2\pi)^4\delta(p_f - p_i)F_{\lambda_1\lambda_2\lambda_3\lambda_4}$.

⁷This convention is not used in [9, 12].

Using these and (A.9), we determine

$$F_{++--}(\beta_Z, \hat{t}, \hat{u}) = F_{++++}(-\beta_Z, \hat{t}, \hat{u}) , \quad (\text{A.12})$$

$$F_{++-0}(\beta_Z, \hat{t}, \hat{u}) = F_{+++0}(-\beta_Z, \hat{t}, \hat{u}) , \quad (\text{A.13})$$

while the remaining 26 amplitudes may be obtained from the ten in (A.11, A.12, A.13), by ($\hat{t} \leftrightarrow \hat{u}$) interchanges or helicity changes; compare (A.6-A.8, A.10).

In SM or any SUSY model, there are two types of contributions to these amplitudes. The first type consists of the one-loop diagrams involving four external legs, like those contributing to the $\gamma\gamma \rightarrow \gamma\gamma$ and $\gamma\gamma \rightarrow \gamma Z$ processes [3, 19, 1, 2]; while the second type includes the Higgs s-channel pole contributions, arising from loops with three external legs generating⁸ $h^0\gamma\gamma$ interactions [9]. To express them economically, we use the notation of [22] for the B_0 , C_0 and D_0 1-loop functions first defined by Passarino and Veltman [13]. For brevity, we introduce the shorthand writing⁹

$$B_0(\hat{s}) \equiv B_0(\hat{s}; m, m) , \quad (\text{A.14})$$

$$C_0(\hat{s}) \equiv C_0(12) = C_0(0, 0, \hat{s}; m, m, m) , \quad (\text{A.15})$$

$$B_Z(\hat{s}) \equiv B_0(\hat{s}) - B_0(m_Z^2 + i\epsilon) , \quad (\text{A.16})$$

$$C_Z(\hat{t}) \equiv C_0(13) \equiv C_0(24) \equiv C_0(0, m_Z^2, \hat{t}; m, m, m) , \quad (\text{A.17})$$

$$C_{ZZ}(\hat{s}) \equiv C_0(34) \equiv C_0(m_Z^2, m_Z^2, \hat{s}; m, m, m) , \quad (\text{A.18})$$

$$D_{ZZ}(\hat{s}, \hat{u}) \equiv D_0(123) \equiv D_0(0, 0, m_Z^2, m_Z^2, \hat{s}, \hat{u}; m, m, m, m) =$$

$$D_{ZZ}(\hat{u}, \hat{s}) \equiv D_0(321) \equiv D_0(m_Z^2, 0, 0, m_Z^2, \hat{u}, \hat{s}; m, m, m, m) , \quad (\text{A.19})$$

$$D_{ZZ}(\hat{s}, \hat{t}) \equiv D_0(213) \equiv D_0(0, 0, m_Z^2, m_Z^2, \hat{s}, \hat{t}; m, m, m, m) =$$

$$D_{ZZ}(\hat{t}, \hat{s}) \equiv D_0(312) \equiv D_0(m_Z^2, 0, 0, m_Z^2, \hat{t}, \hat{s}; m, m, m, m) , \quad (\text{A.20})$$

$$D_{ZZ}(\hat{t}, \hat{u}) \equiv D_0(132) \equiv D_0(0, m_Z^2, 0, m_Z^2, \hat{t}, \hat{u}; m, m, m, m) =$$

$$D_{ZZ}(\hat{u}, \hat{t}) \equiv D_0(231) \equiv D_0(0, m_Z^2, 0, m_Z^2, \hat{u}, \hat{t}; m, m, m, m) \quad (\text{A.21})$$

In diagrams with four external legs, the expressions

$$\tilde{F}(\hat{s}, \hat{t}, \hat{u}) \equiv D_{ZZ}(\hat{s}, \hat{t}) + D_{ZZ}(\hat{s}, \hat{u}) + D_{ZZ}(\hat{t}, \hat{u}) , \quad (\text{A.22})$$

$$E_1(\hat{s}, \hat{t}) \equiv 2\hat{t}_1 C_Z(\hat{t}) - \hat{s}\hat{t} D_{ZZ}(\hat{s}, \hat{t}), \quad (\text{A.23})$$

$$E_2(\hat{t}, \hat{u}) \equiv 2\hat{t}_1 C_Z(\hat{t}) + 2\hat{u}_1 C_Z(\hat{u}) - Y D_{ZZ}(\hat{t}, \hat{u}), \quad (\text{A.24})$$

often appear in the amplitudes below.

The neutral Higgs-pole contribution to the $\gamma\gamma \rightarrow ZZ$ helicity amplitudes, involve the $h^0\gamma\gamma$ interaction generated by spin-1, spin-1/2 or spin-0 loops. They are concisely

⁸Here h^0 denotes any neutral Higgs boson.

⁹The numbers used in the notation of the one loop functions, correspond to the momenta of process (A.1), (taken here as incoming).

described as [18]

$$F_{\lambda_1\lambda_2\lambda_3\lambda_4}^h(\gamma\gamma \rightarrow ZZ) = -\frac{\alpha^2}{2s_W^2 c_W^2} \left\{ \sum_i \mathcal{H}_i(\tau) \right\} \frac{\hat{s}}{\hat{s} - m_h^2 + im_h\Gamma_h} \cdot \frac{(1 + \lambda_1\lambda_2)}{2} \left[(1 + \lambda_3\lambda_4) \frac{\lambda_3\lambda_4}{2} - \frac{1 + \beta_Z^2}{1 - \beta_Z^2} (1 - \lambda_3^2)(1 - \lambda_4^2) \right], \quad (\text{A.25})$$

where the index i runs over the particles in the loop describing the $h^0\gamma\gamma$ vertex, whose spin is (1, 1/2 or 0). In (A.25) the h^0ZZ coupling is taken as in SM; which means *e.g.* that an extra factor $\sin(\beta - \alpha)$ should be introduced in the case of the lightest CP even SUSY Higgs particle. If the interaction Lagrangian of the neutral Higgs to a charged particle pair with spin (1, 1/2, 0) is given by [18]

$$\mathcal{L}_{int} = -\frac{gm_f}{2m_W} \bar{\psi}\psi h^0 + gm_W W_\mu^+ W^{\mu-} h^0 - \frac{gm_{H^\pm}^2}{m_W} H^+ H^- h^0, \quad (\text{A.26})$$

then

$$\mathcal{H}_i(\tau) = N_{ci} Q_i^2 F_i(\tau), \quad (\text{A.27})$$

with

$$F_1(\tau) = \frac{2m_h^2}{\hat{s}} + 3\tau + 3\tau \left(\frac{8}{3} - \frac{2m_h^2}{3\hat{s}} - \tau \right) f(\tau), \quad (\text{A.28})$$

$$F_{1/2}(\tau) = -2\tau[1 + (1 - \tau)f(\tau)], \quad (\text{A.29})$$

$$F_0(\tau) = \tau[1 - \tau f(\tau)], \quad (\text{A.30})$$

where (compare (A.15))

$$\tau = \frac{4m_i^2}{\hat{s}}, \quad f(\tau) = -\frac{\hat{s}}{2} C_0(\hat{s}). \quad (\text{A.31})$$

In (A.27), Q_i is the charge and N_{ci} the colour multiplicity of the particle contributing to $h^0\gamma\gamma$. If more than one neutral Higgs particle with couplings of the type given in (A.26) exists, then a summation over their contributions should be included in (A.25).

We next turn to the contribution from loops in diagrams involving four external legs. It is easiest to describe them by using a non-linear gauge as in [11], for which the same type of particle propagates along the entire loop¹⁰. Thus, the various contributions may simply be described as arising from loops due to a scalar particle, a W boson or a fermion. We give them in this order below.

The scalar particle loop contribution to the helicity amplitudes. We consider the loop contribution due to a scalar particle of mass m , charge Q_S and a definite value of third isospin component t_3^S . In analogy to (A.36) of [3], this contribution is written as

$$F_{\lambda_1\lambda_2\lambda_3\lambda_4}^S(\beta_Z, \hat{t}, \hat{u}) \equiv \alpha^2 Q_S^2 (g_S^Z)^2 A_{\lambda_1\lambda_2\lambda_3\lambda_4}^S(\beta_Z, \hat{t}, \hat{u}; m), \quad (\text{A.32})$$

¹⁰For this gauge, the couplings $\gamma W^\pm \phi^\mp$, $ZW^\pm \phi^\mp$ vanish.

where

$$g_S^Z = \frac{t_3^S - Q_S s_W^2}{s_W c_W} . \quad (\text{A.33})$$

Relations (A.32 , A.33) are directly applicable to a purely L- or R-slepton or squark, while the appropriate mixing should be taken into account in a case like a stop contribution. The scalar contributions to the r.h.s. of (A.32) for the eight basic amplitudes in (A.11), are:

$$\begin{aligned} A_{++++}^S(\beta_Z, \hat{t}, \hat{u}; m) &= -\frac{4\hat{s}_2 Y}{\hat{t}_1 \hat{u}_1 \hat{s}_4} + \frac{4\hat{s}_2 m^2 (\hat{s}\hat{s}_4 - 2Y)}{\hat{s}_4 Y} C_0(\hat{s}) + \frac{4\hat{s}\hat{s}_4 m^2}{Y} C_{ZZ}(\hat{s}) \\ &+ 8m^4 \tilde{F}(\hat{s}, \hat{t}, \hat{u}) + \frac{4[m_Z^2 Y - m^2 \hat{s}\hat{s}_4]}{\hat{s}^2 \hat{s}_4} E_2(\hat{t}, \hat{u}) - \frac{8m_Z^2 m^2 Y}{\hat{s}\hat{s}_4} D_{ZZ}(\hat{t}, \hat{u}) \\ &- 4 \left\{ \frac{m^2 \hat{t}}{Y} E_1(\hat{s}, \hat{t}) + 2m^2 \left(1 + \frac{m_Z^2 \hat{s}_2}{\hat{s}_4 \hat{t}_1} \right) C_Z(\hat{t}) + \frac{m_Z^2 Y}{\hat{s}_4 \hat{t}_1^2} \left(\frac{2\hat{t}}{\hat{s}} - 1 \right) B_Z(\hat{t}) \right. \\ &\left. + \frac{2m_Z^4 m^2}{\hat{s}_4} D_{ZZ}(\hat{s}, \hat{t}) + (\hat{t} \leftrightarrow \hat{u}) \right\} , \quad (\text{A.34}) \end{aligned}$$

$$\begin{aligned} A_{++++}^S(\beta_Z, \hat{t}, \hat{u}; m) &= \frac{4[m_Z^2 (2Y - \hat{s}\hat{s}_4) + \beta_Z \hat{s} Y]}{\hat{s}_4 \hat{t}_1 \hat{u}_1} + \frac{16m_Z^2 m^2}{\hat{s}_4} C_0(\hat{s}) + 8m^4 \tilde{F}(\hat{s}, \hat{t}, \hat{u}) \\ &+ \frac{8Y m^2}{\hat{s}\hat{s}_4} (\hat{s}_2 + \beta_Z \hat{s}) D_{ZZ}(\hat{t}, \hat{u}) - \frac{2[(\hat{s}_2 + \beta_Z \hat{s}) Y - 4\hat{s} m_Z^2 m^2]}{\hat{s}^2 \hat{s}_4} E_2(\hat{t}, \hat{u}) \\ &+ 4 \left\{ \frac{2m^2 m_Z^4}{\hat{s}_4} D_{ZZ}(\hat{s}, \hat{t}) - \frac{[\hat{s}_2 + \beta_Z \hat{s}] [2m_Z^2 Y + \hat{t}_1 (2\hat{t}_1 + \hat{s}) (\hat{t} + m_Z^2)]}{2\hat{s}_4 \hat{t}_1^2} B_Z(\hat{t}) \right. \\ &\left. - \frac{2m^2 [\hat{t}_1 (\hat{t} - \hat{u}) + Y] (\hat{s}_2 + \beta_Z \hat{s})}{\hat{s}_4 \hat{t}_1 \hat{s}} C_Z(\hat{t}) + (\hat{t} \leftrightarrow \hat{u}) \right\} , \quad (\text{A.35}) \end{aligned}$$

$$\begin{aligned} A_{+-++}^S(\beta_Z, \hat{t}, \hat{u}; m) &= -\frac{4\hat{s}_2 Y}{\hat{s}_4 \hat{t}_1 \hat{u}_1} + \frac{4(\hat{s}_4 m^2 + m_Z^4)}{\hat{s}_4 Y} [\hat{s}\hat{s}_2 C_0(\hat{s}) + (\hat{s}\hat{s}_4 - 2Y) C_{ZZ}(\hat{s})] \\ &- \frac{4m^2 \hat{s}_2}{\hat{s}\hat{s}_4} E_2(\hat{t}, \hat{u}) + 8m^4 \tilde{F}(\hat{s}, \hat{t}, \hat{u}) + 4 \left\{ \frac{m_Z^2 (Y + 2\hat{t} m_Z^2)}{\hat{s}_4 \hat{t}_1^2} B_Z(\hat{t}) - \frac{2m^2 \hat{s}_2 \hat{t}}{\hat{s}_4 \hat{t}_1} C_Z(\hat{t}) \right. \\ &\left. + \frac{2m^2 m_Z^4}{\hat{s}_4} D_{ZZ}(\hat{s}, \hat{t}) - \frac{\hat{t} (\hat{s}_4 m^2 + m_Z^4)}{\hat{s}_4 Y} E_1(\hat{s}, \hat{t}) + (\hat{t} \leftrightarrow \hat{u}) \right\} , \quad (\text{A.36}) \end{aligned}$$

$$\begin{aligned} A_{+-00}^S(\beta_Z, \hat{t}, \hat{u}; m) &= -\frac{16m_Z^2 Y}{\hat{s}_4 \hat{t}_1 \hat{u}_1} + \frac{2\hat{s}^2 \hat{s}_2 m_Z^2}{\hat{s}_4 Y} C_0(\hat{s}) + \frac{2\hat{s} m_Z^2}{\hat{s}_4 Y} (\hat{s}\hat{s}_4 - 2Y) C_{ZZ}(\hat{s}) \\ &- \frac{4(\hat{t} - \hat{u})^2 m_Z^2 m^2}{\hat{s}\hat{s}_4} D_{ZZ}(\hat{t}, \hat{u}) - 4 \left\{ \frac{2m_Z^2}{\hat{s}_4 \hat{t}_1^2} (\hat{t}^2 + m_Z^4) B_Z(\hat{t}) - \frac{8m^2 m_Z^2 Y}{\hat{s}_4 \hat{s} \hat{t}_1} C_Z(\hat{t}) \right. \\ &\left. - \frac{\hat{s} m_Z^2 m^2}{\hat{s}_4} D_{ZZ}(\hat{s}, \hat{t}) + \frac{\hat{s} \hat{t} m_Z^2}{2\hat{s}_4 Y} E_1(\hat{s}, \hat{t}) + (\hat{t} \leftrightarrow \hat{u}) \right\} , \quad (\text{A.37}) \end{aligned}$$

$$\begin{aligned}
A_{++00}^S(\beta_Z, \hat{t}, \hat{u}; m) = & -\frac{4m_Z^2 m^2 (\hat{t} - \hat{u})^2}{\hat{s}\hat{s}_4} D_{ZZ}(\hat{t}, \hat{u}) + \frac{16m_Z^2 Y}{\hat{s}_4 \hat{t}_1 \hat{u}_1} + \frac{32m_Z^2 m^2}{\hat{s}_4} C_0(\hat{s}) \\
& + \frac{2m_Z^2 (\hat{t} - \hat{u})^2}{\hat{s}^2 \hat{s}_4} E_2(\hat{t}, \hat{u}) - 4 \left\{ \frac{2m_Z^2}{\hat{s}_4 \hat{s} \hat{t}_1^2} [2m_Z^2 Y + \hat{t}_1 (\hat{t} - \hat{u}) (\hat{t} + m_Z^2)] B_Z(\hat{t}) \right. \\
& \left. - \frac{8m_Z^4 m^2}{\hat{s}_4 \hat{t}_1} C_Z(\hat{t}) - \frac{\hat{s} m_Z^2 m^2}{\hat{s}_4} D_{ZZ}(\hat{s}, \hat{t}) + (\hat{t} \leftrightarrow \hat{u}) \right\}, \tag{A.38}
\end{aligned}$$

$$\begin{aligned}
A_{+++0}^S(\beta_Z, \hat{t}, \hat{u}; m)/\Delta = & -4 \frac{(\hat{t} - \hat{u})}{\hat{s}_4} \left\{ \frac{(1 + \beta_Z) Y}{\hat{t}_1 \hat{u}_1} + 2m^2 C_0(\hat{s}) \right. \\
& \left. - \frac{1}{\hat{s}} \left[\frac{Y(1 + \beta_Z)}{2\hat{s}} + \beta_Z m^2 \right] E_2(\hat{t}, \hat{u}) + \frac{(1 + \beta_Z) m^2 Y}{\hat{s}} D_{ZZ}(\hat{t}, \hat{u}) \right\} \\
& + \frac{4}{\hat{s}_4} \left\{ \frac{(1 + \beta_Z) Y}{\hat{s} \hat{t}_1^2} (\hat{s} m_Z^2 - 2\hat{t} \hat{t}_1) B_Z(\hat{t}) + \frac{2m^2 (1 + \beta_Z) (\hat{t}^2 - m_Z^4 + Y)}{\hat{t}_1} C_Z(\hat{t}) \right. \\
& \left. + m^2 (Y + \hat{t}^2 - m_Z^4) D_{ZZ}(\hat{s}, \hat{t}) - (\hat{t} \leftrightarrow \hat{u}) \right\}, \tag{A.39}
\end{aligned}$$

$$\begin{aligned}
A_{+-+0}^S(\beta_Z, \hat{t}, \hat{u}; m)/\Delta = & -\frac{4(\hat{u} - \hat{t} - \hat{s}\beta_Z) Y}{\hat{s}_4 \hat{t}_1 \hat{u}_1} + \frac{4(\hat{u} - \hat{t} + \hat{s}\beta_Z)}{\hat{s}_4} B_Z(\hat{s}) \\
& + \frac{2\hat{s}}{\hat{s}_4 Y} \left\{ (\hat{t} - \hat{u}) (2m_Z^4 - \hat{s}_2^2) + \beta_Z [4m^2 Y + \hat{s}(\hat{t}^2 + \hat{u}^2)] \right\} C_0(\hat{s}) \\
& + \frac{2\hat{s}\hat{s}_2}{\hat{s}_4 Y} \left\{ (\hat{u} - \hat{t}) \hat{s}_4 + \beta_Z (\hat{s}\hat{s}_4 - 2Y) \right\} C_{ZZ}(\hat{s}) + \frac{4m^2 (\hat{t} - \hat{u})}{\hat{s}\hat{s}_4} E_2(\hat{t}, \hat{u}) \\
& - 4 \left\{ \frac{m_Z^2 Y - \hat{t} \hat{t}_1 (\hat{t} + m_Z^2) + \beta_Z (m_Z^2 Y - \hat{t} \hat{t}_1^2)}{\hat{s}_4 \hat{t}_1^2} B_Z(\hat{t}) \right. \\
& \left. - \frac{[(2m_Z^4 + \hat{t}\hat{s}_2)(2m^2 Y + \hat{s}\hat{t}^2) + \beta_Z \hat{s}\hat{t}(4m^2 Y + \hat{s}\hat{t}^2)]}{2\hat{s}_4 Y \hat{s}} E_1(\hat{s}, \hat{t}) \right. \\
& \left. + \frac{2m^2 [(2m_Z^2 \hat{t}_1 + \hat{s}\hat{t}) Y - \beta_Z \hat{s}^2 \hat{t}^2]}{\hat{s}\hat{s}_4 \hat{t}_1} C_Z(\hat{t}) - (\hat{t} \leftrightarrow \hat{u}, \beta_Z \rightarrow -\beta_Z) \right\}, \tag{A.40}
\end{aligned}$$

$$\begin{aligned}
A_{+--+}^S(\beta_Z, \hat{t}, \hat{u}; m) = & \frac{4[\hat{s}_2 Y + \beta_Z m_Z^2 \hat{s}(\hat{u} - \hat{t})]}{\hat{s}_4 \hat{t}_1 \hat{u}_1} - \frac{4\hat{s}_2 [Y - \hat{s}\{\hat{s}_4 + \beta_Z(\hat{u} - \hat{t})\}]}{\hat{s}_4 Y} B_Z(\hat{s}) \\
& + \frac{4\hat{s}\hat{s}_2}{\hat{s}_4 Y} \left\{ \left[m^2 + \frac{\hat{s}(\hat{s}\hat{s}_4 - Y + m_Z^4)}{2Y} \right] [\hat{s}_4 + \beta_Z(\hat{u} - \hat{t})] - \hat{s}\hat{s}_4 - m_Z^4 \right\} C_0(\hat{s}) \\
& + \frac{4\hat{s}}{Y} \left\{ \left[m^2 + \frac{\hat{t}^2(\hat{t}^2 - m_Z^4 + Y) + \hat{u}^2(\hat{u}^2 - m_Z^4 + Y) + 2Y(\hat{s}_2^2 - m_Z^4)}{2Y\hat{s}_4} \right] [\hat{s}_4 + \beta_Z(\hat{u} - \hat{t})] \right. \\
& \left. + m_Z^4 - \hat{s}_2^2 \right\} C_{ZZ}(\hat{s}) + 8m^2 \left(m^2 - \frac{m_Z^2 Y}{\hat{s}\hat{s}_4} \right) D_{ZZ}(\hat{t}, \hat{u})
\end{aligned}$$

$$\begin{aligned}
& +4 \left\{ -\frac{\hat{t}}{2\hat{s}_4 Y^2} [2m^2 \hat{s}_4 Y + \hat{s} \hat{s}_4 \hat{t}^2 - 2m_Z^4 Y - \beta_Z \hat{s} \hat{t} (\hat{t}^2 - m_Z^4 + Y)] E_1(\hat{s}, \hat{t}) \right. \\
& + \frac{m^2}{\hat{s}_4 Y} [2m^2 \hat{s}_4 Y + \hat{s} \hat{s}_4 \hat{t}^2 - 2m_Z^4 Y - 2\beta_Z \hat{s} \hat{t} (\hat{t}^2 - m_Z^4 + Y)] D_{ZZ}(\hat{s}, \hat{t}) \\
& + \frac{2m^2}{\hat{s}_4 \hat{t}_1} \left[m_Z^2 (\hat{s}_4 + \beta_Z \hat{s}) - \frac{2m_Z^2 Y}{\hat{s}} - \frac{\beta_Z \hat{s} \hat{t} (\hat{t}^2 - m_Z^4)}{Y} \right] C_Z(\hat{t}) \\
& + \left[\left(\frac{m_Z^4 (\hat{t} - \hat{u})}{\hat{s}_4 \hat{t}_1^2} - \frac{1}{2} \right) (1 + \beta_Z) + \frac{m_Z^2}{\hat{s}_4} \left(1 - \frac{2m_Z^4}{\hat{t}_1^2} \right) + \frac{2\hat{t} \beta_Z}{\hat{s}_4} \right. \\
& \left. - \frac{\hat{t}^2}{Y \hat{s}_4} (\hat{s}_4 - \beta_Z (\hat{t} - \hat{u})) \right] B_Z(\hat{t}) + (\hat{t} \leftrightarrow \hat{u}, \beta_Z \rightarrow -\beta_Z) \left. \right\}. \tag{A.41}
\end{aligned}$$

The W loop contribution to the helicity amplitudes are generated in the non-linear gauge [11], by loops involving W , Goldstone bosons and FP ghosts, in diagrams involving four external legs. They have first been presented in [9], and have also been calculated in [10]. Here we give a new expression, using the results in (A.34-A.41). The W -loop contribution to the $\gamma\gamma \rightarrow ZZ$ helicity amplitudes is thus written as

$$F_{\lambda_1 \lambda_2 \lambda_3 \lambda_4}^W(\beta_Z, \hat{t}, \hat{u}) \equiv \frac{\alpha^2}{s_W^2} A_{\lambda_1 \lambda_2 \lambda_3 \lambda_4}^W(\beta_Z, \hat{t}, \hat{u}) \tag{A.42}$$

with

$$\begin{aligned}
A_{\lambda_1 \lambda_2 \lambda_3 \lambda_4}^W(\beta_Z, \hat{t}, \hat{u}) &= \frac{(12c_W^4 - 4c_W^2 + 1)}{4c_W^2} A_{\lambda_1 \lambda_2 \lambda_3 \lambda_4}^S(\beta_Z, \hat{t}, \hat{u}; m_W) \\
&+ \delta_{\lambda_1 \lambda_2 \lambda_3 \lambda_4}^W(\beta_Z, \hat{t}, \hat{u}), \tag{A.43}
\end{aligned}$$

and

$$\delta_{++++}^W(\beta_Z, \hat{t}, \hat{u}) = 0, \tag{A.44}$$

$$\begin{aligned}
\delta_{++++}^W(\beta_Z, \hat{t}, \hat{u}) &= \frac{8m_Z^2 \hat{s} \beta_Z}{\hat{s}_4} C_0(\hat{s}) + \frac{4[2c_W^2 \hat{s}_4 (\hat{s}_2 + \beta_Z \hat{s}) + m_Z^2 (\hat{s}_4 + \beta_Z \hat{s})]}{\hat{s} \hat{s}_4} E_2(\hat{t}, \hat{u}) \\
&- 4c_W^2 [2m_Z^4 + (4m_W^2 - \hat{s})(\hat{s}_2 + \beta_Z \hat{s})] \tilde{F}(\hat{s}, \hat{t}, \hat{u}) \\
&+ \frac{2\hat{s} m_Z^2}{\hat{s}_4} (\hat{s}_4 + \beta_Z \hat{s}_2) [D_{ZZ}(\hat{s}, \hat{t}) + D_{ZZ}(\hat{s}, \hat{u})], \tag{A.45}
\end{aligned}$$

$$\begin{aligned}
\delta_{+-++}^W(\beta_Z, \hat{t}, \hat{u}) &= \frac{4\hat{s}}{\hat{s}_4 Y} [\hat{s}_2 \hat{s}_4 (4m_W^2 - m_Z^2) - 8Y m_W^2] C_0(\hat{s}) \\
&+ \frac{4(4m_W^2 - m_Z^2)(\hat{s} \hat{s}_4 - 2Y)}{Y} C_{ZZ}(\hat{s}) + 8m_W^2 \left[4m_W^2 - m_Z^2 + \frac{2Y}{\hat{s}_4} \right] \tilde{F}(\hat{s}, \hat{t}, \hat{u}) \\
&+ \left\{ \frac{4[4m_W^2 (\hat{t} + m_Z^2)^2 + \hat{t} \hat{s}_4 m_Z^2]}{\hat{s}_4 Y} E_1(\hat{s}, \hat{t}) + \frac{4m_Z^2 Y}{\hat{s}_4} D_{ZZ}(\hat{s}, \hat{t}) + (\hat{t} \leftrightarrow \hat{u}) \right\}, \tag{A.46}
\end{aligned}$$

$$\begin{aligned}
\delta_{+-00}^W(\beta_Z, \hat{t}, \hat{u}) &= \frac{2\hat{s}}{\hat{s}_4 Y} [8m_W^2(\hat{s}_2\hat{s}_4 - 4Y) + \hat{s}_4(\hat{s}_2^2 - 2Y)]C_0(\hat{s}) \\
&+ \frac{2}{Y}(\hat{s}_2 + 8m_W^2)(\hat{s}\hat{s}_4 - 2Y)C_{ZZ}(\hat{s}) + 4m_W^2(\hat{s}_2 + 8m_W^2)\tilde{F}(\hat{s}, \hat{t}, \hat{u}) - \frac{2}{\hat{s}_4}(\hat{s}_4 + 16m_W^2)E_2(\hat{t}, \hat{u}) \\
&+ \left\{ \frac{4\hat{t}_1}{\hat{s}_4 Y} [8m_W^2(Y + (\hat{t} + m_Z^2)^2) - \hat{s}_2\hat{s}_4\hat{t}]C_Z(\hat{t}) + \frac{2}{\hat{s}_4 Y} [8m_W^2(\hat{t}^2\hat{s}\hat{s}_4 - 2Y\hat{t}_1^2) \right. \\
&\left. + \hat{s}((\hat{t}^2 - m_Z^4)^2 - 2m_Z^2\hat{t}^2\hat{s}_4 - \hat{s}\hat{t}Y)]D_{ZZ}(\hat{s}, \hat{t}) + (\hat{t} \leftrightarrow \hat{u}) \right\}, \tag{A.47}
\end{aligned}$$

$$\begin{aligned}
\delta_{++00}^W(\beta_Z, \hat{t}, \hat{u}) &= 4\hat{s}C_0(\hat{s}) - 4m_W^2(\hat{s} + 2m_Z^2 - 8m_W^2)\tilde{F}(\hat{s}, \hat{t}, \hat{u}) \\
&- \frac{4(4m_W^2 - m_Z^2)}{\hat{s}}E_2(\hat{t}, \hat{u}), \tag{A.48}
\end{aligned}$$

$$\begin{aligned}
\delta_{+++0}^W(\beta_Z, \hat{t}, \hat{u})/\Delta &= -\frac{(\hat{t} - \hat{u})(\hat{s}_4 + \beta_Z\hat{s})}{\hat{s}\hat{s}_4} [2\hat{s}C_0(\hat{s}) + E_2(\hat{t}, \hat{u})] \\
&+ \frac{(\hat{s}_4 + \beta_Z\hat{s})}{\hat{s}_4} \left\{ (\hat{t}^2 - m_Z^4 + Y)D_{ZZ}(\hat{s}, \hat{t}) - (\hat{t} \leftrightarrow \hat{u}) \right\}, \tag{A.49}
\end{aligned}$$

$$\begin{aligned}
\delta_{+-+0}^W(\beta_Z, \hat{t}, \hat{u})/\Delta &= -\frac{2}{\hat{s}_4} [(\hat{u} - \hat{t} - \beta_Z\hat{s})\hat{s}_4 + 8c_W^2\hat{s}(\hat{u} - \hat{t} + \beta_Z\hat{s}_4)]C_0(\hat{s}) \\
&+ 16c_W^2(\hat{t} - \hat{u} - \beta_Z\hat{s})C_{ZZ}(\hat{s}) - \frac{64c_W^2m_W^2\beta_Z Y}{\hat{s}_4}\tilde{F}(\hat{s}, \hat{t}, \hat{u}) + \frac{8c_W^2}{\hat{s}_4}Y(\hat{u} - \hat{t} - \beta_Z\hat{s})D_{ZZ}(\hat{t}, \hat{u}) \\
&+ \frac{(\hat{t} - \hat{u} + \beta_Z\hat{s})}{\hat{s}}E_2(\hat{t}, \hat{u}) - \left\{ \frac{(\hat{u} - \hat{t} - \beta_Z\hat{s})}{\hat{s}_4} [2m_Z^4 + 2\hat{t}^2 + \hat{s}\hat{t} - 8c_W^2Y]D_{ZZ}(\hat{s}, \hat{t}) \right. \\
&\left. - \frac{16c_W^2}{\hat{s}_4}(\hat{t} + m_Z^2)(1 + \beta_Z)E_1(\hat{s}, \hat{t}) - (\hat{t} \leftrightarrow \hat{u}, \beta_Z \rightarrow -\beta_Z) \right\}, \tag{A.50}
\end{aligned}$$

$$\begin{aligned}
\delta_{+--+}^W(\beta_Z, \hat{t}, \hat{u}) &= 16c_W^2\hat{s} \left[\frac{\hat{s}_2}{\hat{s}_4}C_0(\hat{s}) + C_{ZZ}(\hat{s}) \right] \\
&+ \frac{4c_W^2}{\hat{s}_4} \left[\hat{s}(\hat{s}_2 + 4m_W^2)(\hat{s}_4 + \beta_Z[\hat{t} - \hat{u}]) - 2Y\hat{s}_2 \right] \tilde{F}(\hat{s}, \hat{t}, \hat{u}) + \left\{ \frac{8c_W^2(\hat{s}_2 + \beta_Z\hat{s})}{\hat{s}_4}E_1(\hat{s}, \hat{t}) \right. \\
&\left. + \frac{2m_Z^2}{\hat{s}_4} \left[\hat{s}(\hat{s}_4 + \beta_Z[\hat{t} - \hat{u}]) - 2Y \right] D_{ZZ}(\hat{s}, \hat{t}) + (\hat{t} \leftrightarrow \hat{u}, \beta_Z \rightarrow -\beta_Z) \right\}, \tag{A.51}
\end{aligned}$$

We have checked that the above W loop contributions to the helicity amplitudes agree with those of [9], except for a minor misprint in the A_{+-+0}^W case¹¹. It should be noticed

¹¹We find that the term $-24c_W^2m_W^2u_1$ in the coefficient of $C(t)$ in (3.14) of [9], should be replaced by $-24c_W^2m_W^2u_1/(ss_4)$.

also that our definitions of \hat{t} and \hat{u} should be interchanged when comparing with [9], and that these authors do not use the JW convention.

The fermion loop contribution. If the effective $Zf\bar{f}$ interaction is written as

$$\mathcal{L}_{Zff} = -eZ^\mu \bar{f}(\gamma_\mu g_{Vf}^Z - \gamma_\mu \gamma_5 g_{Af}^Z)f, \quad (\text{A.52})$$

then the fermion loop contribution (for a fermion of mass m_f), to the $\gamma\gamma \rightarrow ZZ$ helicity amplitude, is given by¹² [12]

$$F_{\lambda_1\lambda_2\lambda_3\lambda_4}^f(\beta_Z, \hat{t}, \hat{u}) \equiv \alpha^2 Q_f^2 \left\{ (g_{Vf}^Z)^2 A_{\lambda_1\lambda_2\lambda_3\lambda_4}^{vf}(\beta_Z, \hat{t}, \hat{u}; m_f) + (g_{Af}^Z)^2 A_{\lambda_1\lambda_2\lambda_3\lambda_4}^{af}(\beta_Z, \hat{t}, \hat{u}; m_f) \right\}. \quad (\text{A.53})$$

In SM, the vector and axial vector couplings for the quarks and leptons are given by (A.52),

$$g_{Vf}^Z = \frac{t_3^f - 2Q_f s_W^2}{2s_W c_W}, \quad g_{Af}^Z = \frac{t_3^f}{2s_W c_W}, \quad (\text{A.54})$$

where t_3^f is the third isospin component of the fermion, and Q_f is its charge.

The vector and axial contributions to the fermion loop amplitudes in (A.53), may be expressed in terms of the A^S amplitudes of (A.34-A.41), by

$$A_{\lambda_1\lambda_2\lambda_3\lambda_4}^{vf}(\beta_Z, \hat{t}, \hat{u}; m_f) = -2A_{\lambda_1\lambda_2\lambda_3\lambda_4}^S(\beta_Z, \hat{t}, \hat{u}; m_f) + \delta_{\lambda_1\lambda_2\lambda_3\lambda_4}^{vf}(\beta_Z, \hat{t}, \hat{u}; m_f), \quad (\text{A.55})$$

$$A_{\lambda_1\lambda_2\lambda_3\lambda_4}^{af}(\beta_Z, \hat{t}, \hat{u}; m_f) = -2A_{\lambda_1\lambda_2\lambda_3\lambda_4}^S(\beta_Z, \hat{t}, \hat{u}; m_f) + \delta_{\lambda_1\lambda_2\lambda_3\lambda_4}^{af}(\beta_Z, \hat{t}, \hat{u}; m_f), \quad (\text{A.56})$$

where

$$\delta_{++++}^{vf}(\beta_Z, \hat{t}, \hat{u}; m_f) = \delta_{++++}^{af}(\beta_Z, \hat{t}, \hat{u}; m_f) = 0, \quad (\text{A.57})$$

$$\delta_{++++}^{vf}(\beta_Z, \hat{t}, \hat{u}; m_f) = 4(\hat{s}_2 + \hat{s}\beta_Z)[m_f^2 \tilde{F}(\hat{s}, \hat{t}, \hat{u}) - \frac{1}{2\hat{s}}E_2(\hat{t}, \hat{u})], \quad (\text{A.58})$$

$$\begin{aligned} \delta_{++++}^{af}(\beta_Z, \hat{t}, \hat{u}; m_f) &= -\frac{8\hat{s}m_f^2}{\hat{s}_4} \left[4\beta_Z C_0(\hat{s}) + (\hat{s}_4 + \beta_Z \hat{s}_2)[D_{ZZ}(\hat{s}, \hat{t}) + D_{ZZ}(\hat{s}, \hat{u})] \right] \\ &+ 4m_f^2(\hat{s}_2 + \hat{s}\beta_Z + 8m_f^2)\tilde{F}(\hat{s}, \hat{t}, \hat{u}) - \frac{2}{\hat{s}} \left[\hat{s}_2 + \hat{s}\beta_Z + \frac{8m_f^2(\hat{s}_4 + \hat{s}\beta_Z)}{\hat{s}_4} \right] E_2(\hat{t}, \hat{u}), \quad (\text{A.59}) \end{aligned}$$

$$\begin{aligned} \delta_{+--+}^{vf}(\beta_Z, \hat{t}, \hat{u}; m_f) &= -\frac{4m_Z^2}{Y} \left[\frac{\hat{s}(\hat{s}_2 \hat{s}_4 - 2Y)}{\hat{s}_4} C_0(\hat{s}) + (\hat{s}\hat{s}_4 - 2Y)C_{ZZ}(\hat{s}) \right] \\ &- \frac{4m_Z^2}{\hat{s}_4 Y} \left[(\hat{t} + m_Z^2)^2 E_1(\hat{s}, \hat{t}) + (\hat{u} + m_Z^2)^2 E_1(\hat{s}, \hat{u}) \right] - 8m_Z^2 m_f^2 \tilde{F}(\hat{s}, \hat{t}, \hat{u}), \quad (\text{A.60}) \end{aligned}$$

¹²As far as the sign of these amplitudes, we agree with [9], apart from the trivial changes introduced by our using of the JW phase conventions.

$$\begin{aligned}
\delta_{+-++}^{af}(\beta_Z, \hat{t}, \hat{u}; m_f) &= 8\hat{s} \left[\frac{\hat{s}_2(4m_f^2 - m_Z^2)}{2Y} + \frac{m_Z^2}{\hat{s}_4} \right] C_0(\hat{s}) + \frac{4(\hat{s}\hat{s}_4 - 2Y)}{Y} (4m_f^2 - m_Z^2) C_{ZZ}(\hat{s}) \\
&+ 8m_f^2(4m_f^2 - m_Z^2) \tilde{F}(\hat{s}, \hat{t}, \hat{u}) + \frac{16m_f^2 Y}{\hat{s}_4} D_{ZZ}(\hat{t}, \hat{u}) \\
&- \frac{4}{Y} \left\{ \left[\frac{m_Z^2(\hat{t} + m_Z^2)^2}{\hat{s}_4} + 4m_f^2 \hat{t} \right] E_1(\hat{s}, \hat{t}) + \left[\frac{m_Z^2(\hat{u} + m_Z^2)^2}{\hat{s}_4} + 4m_f^2 \hat{u} \right] E_1(\hat{s}, \hat{u}) \right\}, \quad (\text{A.61})
\end{aligned}$$

$$\delta_{++00}^{vf}(\beta_Z, \hat{t}, \hat{u}; m_f) = -8m_f^2 m_Z^2 \tilde{F}(\hat{s}, \hat{t}, \hat{u}) + \frac{4m_Z^2}{\hat{s}} E_2(\hat{t}, \hat{u}), \quad (\text{A.62})$$

$$\begin{aligned}
\delta_{++00}^{af}(\beta_Z, \hat{t}, \hat{u}; m_f) &= -8m_f^2 \left(m_Z^2 + \frac{2\hat{s}_2 m_f^2}{m_Z^2} \right) \tilde{F}(\hat{s}, \hat{t}, \hat{u}) \\
&- \frac{4}{\hat{s}} (4m_f^2 - m_Z^2) E_2(\hat{t}, \hat{u}) - \frac{16m_f^2 \hat{s}}{m_Z^2} C_0(\hat{s}), \quad (\text{A.63})
\end{aligned}$$

$$\begin{aligned}
\delta_{+-00}^{vf}(\beta_Z, \hat{t}, \hat{u}; m_f) &= -\frac{4\hat{s}m_Z^2}{\hat{s}_4 Y} (\hat{s}_2 \hat{s}_4 - 4Y) C_0(\hat{s}) - \frac{4m_Z^2}{Y} (\hat{s}\hat{s}_4 - 2Y) C_{ZZ}(\hat{s}) \\
&- 8m_Z^2 m_f^2 \tilde{F}(\hat{s}, \hat{t}, \hat{u}) - \frac{4m_Z^2}{\hat{s}_4 Y} \left[(2\hat{t}^2 + \hat{s}\hat{t} + 2m_Z^4) E_1(\hat{s}, \hat{t}) \right. \\
&\left. + (2\hat{u}^2 + \hat{s}\hat{u} + 2m_Z^4) E_1(\hat{s}, \hat{u}) \right], \quad (\text{A.64})
\end{aligned}$$

$$\begin{aligned}
\delta_{+-00}^{af}(\beta_Z, \hat{t}, \hat{u}; m_f) &= -\frac{8m_f^2}{m_Z^2} \left\{ \hat{s} \left(\frac{\hat{s}_2^2}{Y} - 2 \right) C_0(\hat{s}) + \hat{s}_2 \left(\frac{\hat{s}\hat{s}_4}{Y} - 2 \right) C_{ZZ}(\hat{s}) - \frac{4m_Z^2 Y}{\hat{s}_4} D_{ZZ}(\hat{t}, \hat{u}) \right. \\
&+ \frac{(\hat{t}^2 + m_Z^4)}{Y} E_1(\hat{s}, \hat{t}) + \frac{(\hat{u}^2 + m_Z^4)}{Y} E_1(\hat{s}, \hat{u}) + (2\hat{s}_2 m_f^2 + m_Z^4) \tilde{F}(\hat{s}, \hat{t}, \hat{u}) \left. \right\} \\
&- \frac{4m_Z^2}{Y} \left[\frac{\hat{s}}{\hat{s}_4} (\hat{s}_2 \hat{s}_4 - 4Y) C_0(\hat{s}) + (\hat{s}\hat{s}_4 - 2Y) C_{ZZ}(\hat{s}) + \frac{(2\hat{t}^2 + \hat{s}\hat{t} + 2m_Z^4)}{\hat{s}_4} E_1(\hat{s}, \hat{t}) \right. \\
&\left. + \frac{(2\hat{u}^2 + \hat{s}\hat{u} + 2m_Z^4)}{\hat{s}_4} E_1(\hat{s}, \hat{u}) \right], \quad (\text{A.65})
\end{aligned}$$

$$\delta_{++++}^{vf}(\beta_Z, \hat{t}, \hat{u}; m_f) = 0, \quad (\text{A.66})$$

$$\begin{aligned}
\delta_{++++}^{af}(\beta_Z, \hat{t}, \hat{u}; m_f) / \Delta &= -\frac{4(\hat{s}_4 + \beta_Z \hat{s}) m_f^2}{\hat{s}_4 m_Z^2} \left\{ (\hat{u} - \hat{t}) \left[2C_0(\hat{s}) + \frac{1}{\hat{s}} E_2(\hat{t}, \hat{u}) \right] \right. \\
&\left. - (\hat{s}\hat{t} - 2m_Z^2 \hat{t}_1) D_{ZZ}(\hat{s}, \hat{t}) + (\hat{s}\hat{u} - 2m_Z^2 \hat{u}_1) D_{ZZ}(\hat{s}, \hat{u}) \right\}, \quad (\text{A.67})
\end{aligned}$$

$$\delta_{+-+0}^{vf}(\beta_Z, \hat{t}, \hat{u}; m_f) / \Delta = -\frac{4\hat{s}}{\hat{s}_4} (\hat{t} - \hat{u} - \beta_Z \hat{s}_4) C_0(\hat{s}) - 4(\hat{t} - \hat{u} - \beta_Z \hat{s}) C_{ZZ}(\hat{s})$$

$$\begin{aligned}
& + \frac{16\beta_Z m_f^2 Y}{\hat{s}_4} \tilde{F}(\hat{s}, \hat{t}, \hat{u}) - \frac{4(1 + \beta_Z)(\hat{t} + m_Z^2)}{\hat{s}_4} E_1(\hat{s}, \hat{t}) \\
& + \frac{4(1 - \beta_Z)(\hat{u} + m_Z^2)}{\hat{s}_4} E_1(\hat{s}, \hat{u}) , \tag{A.68}
\end{aligned}$$

$$\begin{aligned}
\delta_{+-+0}^{af}(\beta_Z, \hat{t}, \hat{u}; m_f)/\Delta &= -\frac{4m_f^2}{m_Z^2 \hat{s}} (\hat{t} - \hat{u} + \beta_Z \hat{s}) \left\{ 2\hat{s} C_0(\hat{s}) + E_1(\hat{s}, \hat{t}) + E_1(\hat{s}, \hat{u}) \right. \\
& + \left. \frac{(\hat{s} + 4m_Z^2)Y}{\hat{s}_4} D_{ZZ}(\hat{t}, \hat{u}) \right\} + \frac{16\beta_Z m_f^2 Y}{\hat{s}_4} \tilde{F}(\hat{s}, \hat{t}, \hat{u}) - \frac{4\hat{s}}{\hat{s}_4} (\hat{t} - \hat{u} - \beta_Z \hat{s}_4) C_0(\hat{s}) \\
& - 4(\hat{t} - \hat{u} - \beta_Z \hat{s}) C_{ZZ}(\hat{s}) - \frac{4(1 + \beta_Z)(\hat{t} + m_Z^2)}{\hat{s}_4} E_1(\hat{s}, \hat{t}) \\
& + \frac{4(1 - \beta_Z)(\hat{u} + m_Z^2)}{\hat{s}_4} E_1(\hat{s}, \hat{u}) , \tag{A.69}
\end{aligned}$$

$$\begin{aligned}
\delta_{+--+}^{vf}(\beta_Z, \hat{t}, \hat{u}; m_f) &= -4\hat{s} \left[\frac{\hat{s}_2}{\hat{s}_4} C_0(\hat{s}) + C_{ZZ}(\hat{s}) \right] - \frac{2}{\hat{s}_4} \left[(\hat{s}_2 + \beta_Z \hat{s}) E_1(\hat{s}, \hat{t}) \right. \\
& + \left. (\hat{s}_2 - \beta_Z \hat{s}) E_1(\hat{s}, \hat{u}) \right] - \frac{4\hat{s}m_f^2}{\hat{s}_4} [\hat{s}_4 + \beta_Z(\hat{t} - \hat{u})] \tilde{F}(\hat{s}, \hat{t}, \hat{u}) , \tag{A.70}
\end{aligned}$$

$$\begin{aligned}
\delta_{+--+}^{af}(\beta_Z, \hat{t}, \hat{u}; m_f) &= -4\hat{s} \left[\frac{\hat{s}_2}{\hat{s}_4} C_0(\hat{s}) + C_{ZZ}(\hat{s}) \right] - \frac{2}{\hat{s}_4} \left[(\hat{s}_2 + \beta_Z \hat{s}) E_1(\hat{s}, \hat{t}) + (\hat{s}_2 - \beta_Z \hat{s}) E_1(\hat{s}, \hat{u}) \right] \\
& - \frac{4\hat{s}m_f^2}{\hat{s}_4} [\hat{s}_4 + \beta_Z(\hat{t} - \hat{u})] [\tilde{F}(\hat{s}, \hat{t}, \hat{u}) - 2D_{ZZ}(\hat{t}, \hat{u})] - \frac{16m_f^2 Y}{\hat{s}_4} D_{ZZ}(\hat{t}, \hat{u}) . \tag{A.71}
\end{aligned}$$

We have checked that the fermion loop results in (A.52- A.71) agree with those of [12], apart from the overall sign, provided that the replacement

$$\Delta_{ref.[12]} \longrightarrow -\frac{2}{\hat{s}} \Delta \tag{A.72}$$

is made¹³. In addition to this, it should be remembered that our definitions of \hat{t} and \hat{u} should be interchanged when comparing with [12], and that these authors do not use the JW convention.

¹³A factor of \hat{s} is apparently missing in the first term within the curly brackets in Eqs.(3.14) of [12].

Appendix B: The asymptotic $\gamma\gamma \rightarrow ZZ$ amplitudes in SM.

Since the expressions in Appendix A for the $\gamma\gamma \rightarrow ZZ$ helicity amplitudes are rather complicated, it would be useful to quote their asymptotic expressions involving logarithmic functions only. To this purpose, we need the asymptotic expressions for the Passarino-Veltman functions in (A.15, A.16),

$$B_Z(\hat{s}) \simeq -\ln\left(\frac{-\hat{s} - i\epsilon}{-m_Z^2 - i\epsilon}\right) , \quad (\text{B.1})$$

$$C_0(\hat{s}) = \frac{1}{2\hat{s}} \left[\ln\left(\frac{\sqrt{1 - (4m^2/\hat{s})} + i\epsilon - 1}{\sqrt{1 - (4m^2/\hat{s})} + i\epsilon + 1}\right) \right]^2 \simeq \frac{1}{2\hat{s}} \left[\ln\left(\frac{-\hat{s} - i\epsilon}{m^2}\right) \right]^2 , \quad (\text{B.2})$$

which should be valid for $|\hat{s}| \gg (m^2, m_Z^2)$, [23, 1, 3].

For the 1-loop functions $C_Z(\hat{s})$, C_{ZZ} and D_{ZZ} , containing one or two legs at the Z -mass shell, the asymptotic expressions depend also on the threshold singularity through [23]

$$a_Z \equiv \sqrt{1 - \frac{4m^2}{m_Z^2} + i\epsilon} . \quad (\text{B.3})$$

Taking then $|\hat{s}| \gg (m^2, m_Z^2)$, and using the definition

$$\tilde{a}_Z \equiv \pi^2 - \left[\ln\left(\frac{1+a_Z}{2}\right) - \ln\left(\frac{1-a_Z}{2}\right) \right]^2 + 2i\pi \left[\ln\left(\frac{1+a_Z}{2}\right) - \ln\left(\frac{1-a_Z}{2}\right) \right] , \quad (\text{B.4})$$

we get

$$C_Z(\hat{s}) \simeq \frac{1}{\hat{s}} \left\{ \frac{1}{2} \ln^2\left(\frac{-\hat{s} - i\epsilon}{m^2}\right) + \frac{\tilde{a}_Z}{2} \right\} , \quad (\text{B.5})$$

$$C_{ZZ}(\hat{s}) \simeq \frac{1}{\hat{s}} \left\{ \frac{1}{2} \ln^2\left(\frac{-\hat{s} - i\epsilon}{m^2}\right) + \tilde{a}_Z \right\} , \quad (\text{B.6})$$

while for $(|\hat{s}|, |\hat{t}|) \gg (m^2, m_Z^2)$, we get [23]

$$D_{ZZ}(\hat{s}, \hat{t}) \simeq \frac{2}{\hat{s}\hat{t}} \left\{ \ln\left(\frac{-\hat{s} - i\epsilon}{m^2}\right) \ln\left(\frac{-\hat{t} - i\epsilon}{m^2}\right) - \frac{\pi^2}{2} + \tilde{a}_Z \right\} . \quad (\text{B.7})$$

The principal value of the logarithms is understood in (B.1, B.2, B.5-B.7), with the cuts along the negative real axis. These asymptotic expressions should be quite accurate in the indicated regions, except in the case where $m_Z \gg m$; which leads to $a_Z \rightarrow 1$ and $|\tilde{a}_Z| \rightarrow \infty$, disturbing (B.5-B.7). Thus, for *e.g.* $C_{ZZ}(\hat{s})$ at $\hat{s} = -m_Z^4/m^2(1 - 4m^2/m_Z^2) \gg m_Z^2$, the exact expression in (A.18) differs considerably from the asymptotic result of (B.6). Nevertheless, it is shown below that these mass singularities cancel in the asymptotic behaviour of the physical $\gamma\gamma \rightarrow ZZ$ amplitudes. A similar property has also been observed for the $\gamma\gamma \rightarrow \gamma Z$ case [3]. This cancellation should be a consequence of gauge invariance and a reflection of the fact that although some single log imaginary terms remain in

the asymptotic expressions for the physical amplitudes of these processes, there are no overlapping soft and collinear singularities which would have led to double-log Sudakov type terms [24]. We come back to this at the end of this Appendix.

Before turning to this though, we remark on the basis of (B.5-B.7), that for $(\hat{s} \sim |\hat{t}| \sim |u|) \gg (m_Z^2, m^2)$, the corresponding asymptotic expressions for the functions in (A.22-A.24) are

$$\begin{aligned} \tilde{F}(\hat{s}, \hat{t}, \hat{u}) &\simeq \frac{2}{\hat{s}\hat{u}} \ln\left(\frac{-\hat{s}-i\epsilon}{m^2}\right) \ln\left(\frac{-\hat{u}-i\epsilon}{m^2}\right) + \frac{2}{\hat{s}\hat{t}} \ln\left(\frac{-\hat{s}-i\epsilon}{m^2}\right) \ln\left(\frac{-\hat{t}-i\epsilon}{m^2}\right) \\ &\quad + \frac{2}{\hat{t}\hat{u}} \ln\left(\frac{-\hat{t}-i\epsilon}{m^2}\right) \ln\left(\frac{-\hat{u}-i\epsilon}{m^2}\right), \end{aligned} \quad (\text{B.8})$$

$$E_1(\hat{s}, \hat{t}) \simeq \pi^2 - \tilde{a}_Z + \ln^2\left(\frac{-\hat{t}-i\epsilon}{m^2}\right) - 2 \ln\left(\frac{-\hat{s}-i\epsilon}{m^2}\right) \ln\left(\frac{-\hat{t}-i\epsilon}{m^2}\right), \quad (\text{B.9})$$

$$E_2(\hat{t}, \hat{u}) \simeq \pi^2 + \left[\ln\left(\frac{-\hat{t}-i\epsilon}{m^2}\right) - \ln\left(\frac{-\hat{u}-i\epsilon}{m^2}\right) \right]^2. \quad (\text{B.10})$$

In the remaining part of this Appendix we give the asymptotic expressions for the ten amplitudes in (A.11, A.12, A.13), by neglecting terms of $O(m_Z^2/\hat{s}, m_Z m/\hat{s}, m^2/\hat{s})$. These should hold in the region

$$\hat{s} \sim |\hat{t}| \sim |\hat{u}| \gg (m_Z^2, m^2) \quad (\text{B.11})$$

where m is the mass of the scalar or fermion particle circulating in the loop. Thus, for the scalar loop contributions, using (A.32) and (A.34-A.41), we find

$$A_{++++}^S \simeq 4 - \frac{4\hat{u}\hat{t}}{\hat{s}^2} \left[\ln^2\left|\frac{\hat{t}}{\hat{u}}\right| + \pi^2 \right] + \frac{4(\hat{t}-\hat{u})}{\hat{s}} \ln\left|\frac{\hat{t}}{\hat{u}}\right|, \quad (\text{B.12})$$

$$A_{+--+}^S \simeq 4 - \frac{4\hat{s}\hat{t}}{\hat{u}^2} \left[\ln^2\left|\frac{\hat{s}}{\hat{t}}\right| - 2i\pi \ln\left|\frac{\hat{s}}{\hat{t}}\right| \right] + \frac{4(\hat{s}-\hat{t})}{\hat{u}} \left[\ln\left|\frac{\hat{s}}{\hat{t}}\right| - i\pi \right], \quad (\text{B.13})$$

$$A_{++++0}^S \simeq \sqrt{\frac{\hat{s}m_Z^2}{2\hat{u}\hat{t}}} \left\{ -\frac{8(\hat{t}-\hat{u})}{\hat{s}} + \frac{4(\hat{t}-\hat{u})\hat{t}\hat{u}}{\hat{s}^3} \left[\ln^2\left|\frac{\hat{t}}{\hat{u}}\right| + \pi^2 \right] + \frac{16\hat{u}\hat{t}}{\hat{s}^2} \ln\left|\frac{\hat{t}}{\hat{u}}\right| \right\}, \quad (\text{B.14})$$

$$A_{+--+0}^S \simeq \sqrt{\frac{\hat{s}m_Z^2}{2\hat{u}\hat{t}}} \left\{ -\frac{8\hat{u}}{\hat{s}} + \frac{4\hat{t}}{\hat{u}} \left[\ln^2\left|\frac{\hat{s}}{\hat{t}}\right| - 2i\pi \ln\left|\frac{\hat{s}}{\hat{t}}\right| \right] + \frac{8\hat{t}}{\hat{s}} \left[\ln\left|\frac{\hat{s}}{\hat{t}}\right| - i\pi \right] \right\}, \quad (\text{B.15})$$

while the rest are found to be very small, *i.e.*

$$A_{++++-}^S \simeq A_{+---}^S \simeq A_{-+++}^S \simeq -4, \quad (\text{B.16})$$

$$A_{+-00}^S \simeq A_{+00}^S \simeq A_{++-0}^S \simeq 0. \quad (\text{B.17})$$

The corresponding asymptotic expressions for the W loop contributions are given by (A.42, A.43) and the relations

$$\delta_{++++}^W \simeq 16c_W^2 \left\{ \ln^2\left|\frac{\hat{t}}{\hat{u}}\right| + \pi^2 + \frac{\hat{s}}{\hat{u}} \ln\left|\frac{\hat{u}}{m_W^2}\right| \ln\left|\frac{\hat{s}}{\hat{t}}\right| \right\}$$

$$+ \frac{\hat{s}}{\hat{t}} \ln \left| \frac{\hat{t}}{m_W^2} \right| \ln \left| \frac{\hat{s}}{\hat{u}} \right| - i\pi \left[\frac{\hat{s}}{\hat{u}} \ln \left| \frac{\hat{u}}{m_W^2} \right| + \frac{\hat{s}}{\hat{t}} \ln \left| \frac{\hat{t}}{m_W^2} \right| \right] \Big\} , \quad (\text{B.18})$$

$$\begin{aligned} \delta_{+-+-}^W &\simeq 16c_W^2 \left\{ \ln^2 \left| \frac{\hat{t}}{\hat{s}} \right| + \frac{\hat{u}}{\hat{t}} \ln \left| \frac{\hat{t}}{m_W^2} \right| \ln \left| \frac{\hat{u}}{\hat{s}} \right| + \frac{\hat{u}}{\hat{s}} \ln \left| \frac{\hat{s}}{m_W^2} \right| \ln \left| \frac{\hat{u}}{\hat{t}} \right| \right. \\ &\quad \left. + i\pi \left[\frac{\hat{u}}{\hat{t}} \ln \left(\frac{\hat{s}}{m_W^2} \right) - \frac{\hat{u}}{\hat{s}} \ln \left| \frac{\hat{u}}{\hat{s}} \right| - \frac{(\hat{s}^2 + \hat{t}^2)}{\hat{s}\hat{t}} \ln \left| \frac{\hat{t}}{\hat{s}} \right| \right] \right\} , \quad (\text{B.19}) \end{aligned}$$

$$\begin{aligned} \delta_{+-00}^W &\simeq -2 \left[\ln^2 \left| \frac{\hat{t}}{\hat{u}} \right| + \frac{\hat{s}}{\hat{u}} \ln^2 \left| \frac{\hat{t}}{\hat{s}} \right| + \frac{\hat{s}}{\hat{t}} \ln^2 \left| \frac{\hat{u}}{\hat{s}} \right| \right] - \frac{4}{\hat{s}} \ln \left(\frac{\hat{s}}{m_W^2} \right) \left[\hat{t} \ln \left| \frac{\hat{t}}{\hat{s}} \right| + \hat{u} \ln \left| \frac{\hat{u}}{\hat{s}} \right| \right] \\ &\quad + i4\pi \left\{ \ln \left(\frac{\hat{s}}{m_W^2} \right) + \left(1 - \frac{\hat{t}^2}{\hat{s}\hat{u}} \right) \ln \left| \frac{\hat{t}}{\hat{s}} \right| + \left(1 - \frac{\hat{u}^2}{\hat{s}\hat{t}} \right) \ln \left| \frac{\hat{u}}{\hat{s}} \right| \right\} , \quad (\text{B.20}) \end{aligned}$$

$$\delta_{++00}^W \simeq 2 \ln^2 \left(\frac{\hat{s}}{m_W^2} \right) - 2\pi^2 - i4\pi \ln \left(\frac{\hat{s}}{m_W^2} \right) , \quad (\text{B.21})$$

$$\begin{aligned} \delta_{++++}^W &\simeq \sqrt{\frac{\hat{s}m_Z^2}{2\hat{u}\hat{t}}} \left\{ -\frac{2(\hat{t} - \hat{u})}{\hat{s}} \left[\ln^2 \left(\frac{\hat{s}}{m_W^2} \right) + \ln^2 \left| \frac{\hat{t}}{\hat{u}} \right| - i2\pi \ln \left(\frac{\hat{s}}{m_W^2} \right) \right] \right. \\ &\quad \left. - 4 \left[\ln \left(\frac{\hat{s}}{m_W^2} \right) - i\pi \right] \ln \left| \frac{\hat{t}}{\hat{u}} \right| \right\} , \quad (\text{B.22}) \end{aligned}$$

$$\begin{aligned} \delta_{+--+}^W &\simeq \sqrt{\frac{\hat{s}m_Z^2}{2\hat{u}\hat{t}}} \left\{ \left(-\frac{2\hat{u}}{\hat{s}} + 32c_W^2 \frac{\hat{t}}{\hat{s}} \right) \left[\ln^2 \left(\frac{\hat{s}}{m_W^2} \right) - i2\pi \ln \left(\frac{\hat{s}}{m_W^2} \right) \right] \right. \\ &\quad + 32c_W^2 \left[\frac{\hat{u}}{\hat{s}} \ln \left| \frac{\hat{t}}{m_W^2} \right| \ln \left| \frac{\hat{u}}{m_W^2} \right| + \frac{\hat{t}}{\hat{s}} \ln^2 \left| \frac{\hat{t}}{m_W^2} \right| \right] - \frac{2\hat{u}}{\hat{s}} \ln^2 \left| \frac{\hat{t}}{\hat{u}} \right| \\ &\quad + \left[-\frac{4\hat{u}(\hat{t} - \hat{u})}{\hat{s}^2} + 32c_W^2 \frac{(\hat{t}^2 + \hat{s}^2)}{\hat{s}^2} \right] \left[\ln \left(\frac{\hat{s}}{m_W^2} \right) - i\pi \right] \ln \left| \frac{\hat{t}}{m_W^2} \right| \\ &\quad \left. - \frac{4\hat{u}}{\hat{s}^2} (\hat{u} - \hat{t} - 8c_W^2 \hat{t}) \left[\ln \left(\frac{\hat{s}}{m_W^2} \right) - i\pi \right] \ln \left| \frac{\hat{u}}{m_W^2} \right| \right\} , \quad (\text{B.23}) \end{aligned}$$

$$\delta_{++++}^W \simeq \delta_{+--+}^W \simeq \delta_{+--+}^W \simeq \delta_{+--+}^W \simeq 0 . \quad (\text{B.24})$$

The asymptotic expressions for the fermion loop contributions may be expressed from (A.53, A.55, A.56) and the results

$$\delta_{++++}^{vf} \simeq \delta_{++++}^{af} \simeq -4 \left\{ \ln^2 \left| \frac{\hat{u}}{\hat{t}} \right| + \pi^2 \right\} , \quad (\text{B.25})$$

$$\delta_{+--+}^{vf} \simeq \delta_{+--+}^{af} \simeq -4 \left\{ \ln^2 \left| \frac{\hat{s}}{\hat{t}} \right| - i2\pi \ln \left| \frac{\hat{s}}{\hat{t}} \right| \right\} , \quad (\text{B.26})$$

$$\delta_{+-00}^{vf} \simeq \delta_{++00}^{vf} \simeq \delta_{++++}^{vf} \simeq 0 , \quad (\text{B.27})$$

$$\delta_{+-00}^{af} \simeq -\frac{8m_Z^2}{m_Z^2} \left\{ \frac{\hat{t}}{\hat{u}} \left[\ln^2 \left| \frac{\hat{t}}{\hat{s}} \right| + i2\pi \ln \left| \frac{\hat{t}}{\hat{s}} \right| \right] + \frac{\hat{u}}{\hat{t}} \left[\ln^2 \left| \frac{\hat{u}}{\hat{s}} \right| + i2\pi \ln \left| \frac{\hat{u}}{\hat{s}} \right| \right] \right\} , \quad (\text{B.28})$$

$$\delta_{++++0}^{af} \simeq -\frac{8m^2}{m_Z^2} \left\{ \ln^2 \left(\frac{\hat{s}}{m^2} \right) - \pi^2 - i2\pi \ln \left(\frac{\hat{s}}{m^2} \right) \right\}, \quad (\text{B.29})$$

$$\begin{aligned} \delta_{++++0}^{af} &\simeq -\sqrt{\frac{\hat{s}m_Z^2}{2\hat{u}\hat{t}}} \frac{8m^2}{m_Z^2} \left\{ \frac{(\hat{u}-\hat{t})}{\hat{s}} \left[\ln^2 \left(\frac{\hat{s}}{m^2} \right) - i2\pi \ln \left(\frac{\hat{s}}{m^2} \right) + \ln^2 \left| \frac{\hat{t}}{\hat{u}} \right| \right] \right. \\ &\quad \left. - 2 \ln \left(\frac{\hat{s}}{m^2} \right) \ln \left| \frac{\hat{t}}{\hat{u}} \right| + i2\pi \ln \left| \frac{\hat{t}}{\hat{u}} \right| \right\}, \end{aligned} \quad (\text{B.30})$$

$$\delta_{+--+0}^{vf} \simeq -\sqrt{\frac{\hat{s}m_Z^2}{2\hat{u}\hat{t}}} \frac{8\hat{t}}{\hat{s}} \left\{ \ln^2 \left| \frac{\hat{s}}{\hat{t}} \right| - i2\pi \ln \left| \frac{\hat{s}}{\hat{t}} \right| \right\}, \quad (\text{B.31})$$

$$\begin{aligned} \delta_{+--+0}^{af} &\simeq -\sqrt{\frac{\hat{s}m_Z^2}{2\hat{u}\hat{t}}} \frac{8\hat{t}}{\hat{s}} \left\{ \ln^2 \left| \frac{\hat{s}}{\hat{t}} \right| - i2\pi \ln \left| \frac{\hat{s}}{\hat{t}} \right| \right\} \\ &\quad + \sqrt{\frac{\hat{s}m_Z^2}{2\hat{u}\hat{t}}} \frac{8m^2\hat{u}}{m_Z^2\hat{s}} \left\{ \ln^2 \left(\frac{\hat{s}m^2}{\hat{t}\hat{u}} \right) - i2\pi \ln \left(\frac{\hat{s}m^2}{\hat{t}\hat{u}} \right) \right\}, \end{aligned} \quad (\text{B.32})$$

$$\delta_{++++-}^{vf} \simeq \delta_{++++-}^{af} \simeq \delta_{+--+ -}^{vf} \simeq \delta_{+--+ -}^{af} \simeq \delta_{+--+ +}^{vf} \simeq \delta_{+--+ +}^{af} \simeq \delta_{+--+ 0}^{vf} \simeq \delta_{+--+ 0}^{af} \simeq 0. \quad (\text{B.33})$$

As promised, the asymptotic expressions of the helicity amplitudes derived from the preceding formulae, do not depend on the parameter a_Z of (B.3, B.4) entering the Passarino-Veltman functions in (B.5-B.7, B.9). We also notice that the Sudakov-type log-squared terms in (B.2, B.5 - B.10) cancel out, when substituted to these amplitudes, because of Bose symmetry. Therefore, in the asymptotic region indicated in (B.11), the only large contributions come from the single-logarithm imaginary terms appearing in δ_{++++}^W and δ_{+--+}^W ; compare (B.18 B.19). These terms are the only ones which increase (logarithmically) with \hat{s} .

References

- [1] G.J. Gounaris, P.I. Porfyriadis, F.M. Renard, hep-ph/9902230, Eur. Phys. J. **C9** (1999) 673.
- [2] G.J. Gounaris, P.I. Porfyriadis, F.M. Renard, hep-ph/9812378, Phys. Lett. **B452** (1999) 76. Please notice that a factor i has been forgotten in front of the second term in Eq.(4) of this paper.
- [3] G.J. Gounaris, J. Layssac, P.I. Porfyriadis and F.M. Renard, Eur.Phys.Jour.**C10**(1999)(499).
- [4] Opportunities and Requirements for Experimentation at a Very High Energy e^+e^- Collider, SLAC-329(1928); Proc. Workshops on Japan Linear Collider, KEK Reports, 90-2, 91-10 and 92-16; P.M. Zerwas, DESY 93-112, Aug. 1993; Proc. of the Workshop on e^+e^- Collisions at 500 GeV: The Physics Potential, DESY 92-123A,B,(1992), C(1993), D(1994), E(1997) ed. P. Zerwas; E. Accomando *et.al.* Phys. Rep. **C299** (299) 1998.
- [5] I.F. Ginzburg, G.L. Kotkin, V.G. Serbo and V.I. Telnov, Nucl. Instr. and Meth. **205**, 47 (1983); I.F. Ginzburg, G.L. Kotkin, V.G. Serbo, S.L. Panfil and V.I. Telnov, Nucl. Instr. and Meth. **219**(1984)5; J.H. Kühn, E.Mirkes and J. Steegborn, Z. f. Phys. **C57** (1993) 615;
- [6] R. Brinkman *et.al.* hep-ex/9707017; V. Telnov hep-ex/9802003, hep-ex/9805002, hep-ex/9908005; I.F. Ginzburg, hep-ph/9907549.
- [7] H. Davoudiasl, hep-ph/9904425; K. Cheung, hep-ph/9904266; T.G. Rizzo, hep-ph/9907401.
- [8] I. Antoniadis, K. Benakli and M. Quirós, hep-ph/9905311.
- [9] G. Jikia, Nucl. Phys. **B405** (1993) 24, Phys. Lett. **B298** (1993) 224.
- [10] B. Bajc Phys. Rev. **D48** (1993) R1907; M.S. Berger Phys. Rev. **D48** (1993) 5121.
- [11] D.A. Dicus and C. Kao, Phys. Rev. **D49** (1994) 1265.
- [12] E.W.N. Glover and J.J. van der Bij, Nucl. Phys. **B321** (1989) 561.
- [13] G. Passarino and M. Veltman, Nucl. Phys. **B160** (1979) 151.
- [14] For reviews of SUSY couplings see *e.g.* H. Nilles Phys. Rep. **C110** (1984) 1; H.E. Haber, G.L. Kane, Phys. Rep. **C117** (1985) 75.
- [15] S.Y. Choi, A. Djouadi, H. Dreiner, J. Kalinowski and P.M. Zerwas, hep-ph/9806279, Eur. Phys. J. **C7** (1999) 123.

- [16] G.J. van Oldenborgh and J.A.M. Vermaseren, *Z. f. Phys.* **C46** (1990) 425; G.J. van Oldenborgh "FF: A package to evaluate one loop Feynman diagrams" *Comput. Phys. Commun.* **66** (1991) 1.
- [17] C. Boehm, A. Djouadi and Y. Mambrini, hep-ph/9907428.
- [18] J.F. Gunion, H.E. Haber, G. Kane and S. Dawson, "The Higgs Hunter's Guide", Addison-Wesley, Redwood City (1990).
- [19] G. Jikia and A. Tkabladze, *Phys. Lett.* **B332** (1994) 441.
- [20] E.W.N. Glover and J.J. van der Bij, *Nucl. Phys.* **B313** (1989) 237; M.L. Lausen, K.O. Mikaelian and M.A. Samuel, *Phys. Rev.* **D23** (1981) 2795; E.W. N. Glover and A.G. Morgan, *Z. f. Phys.* **C60** (1993) 175; M. Baillargeon and F. Boudjema, *Phys. Lett.* **B272** (1991) 158; F.-X. Dong, X.-D. Jiang and X.-J. Zhou, *Phys. Rev.* **D46** (1992) 5074; M.-z. Yang and X.j. Zhou, *Phys. Rev.* **D52** (1995) 5018.
- [21] R. Karplus and M. Neuman, *Phys. Rev.* **80** (1950) 380; *Phys. Rev.* **83** (1951) 776; B. De Tollis, *Nuovo Cim.* **35** (1965) 1182; V. Constantini, B. De Tollis and G. Pistoni, *Nuovo Cim.* **A2** (1971) 733; G. Jikia and A. Tkabladze, *Phys. Lett.* **B323** (1994) 453.
- [22] K. Hagiwara, S. Matsumoto, D. Haidt and C.S. Kim, *Z. f. Phys.* **C64** (1995) 559.
- [23] M. Roth and A. Denner *Nucl. Phys.* **B479** (1996) 495, hep-ph/9605420; A. Denner and S. Dittmaier, hep-ph/9812411, *Eur. Phys. J.* **C9** (1999) 425.
- [24] see *e.g.* G. Sterman, Lectures at the Theoretical Advanced Study Institute *QCD and Beyond*, Boulder, Co., June 1995, hep-ph/9606312.

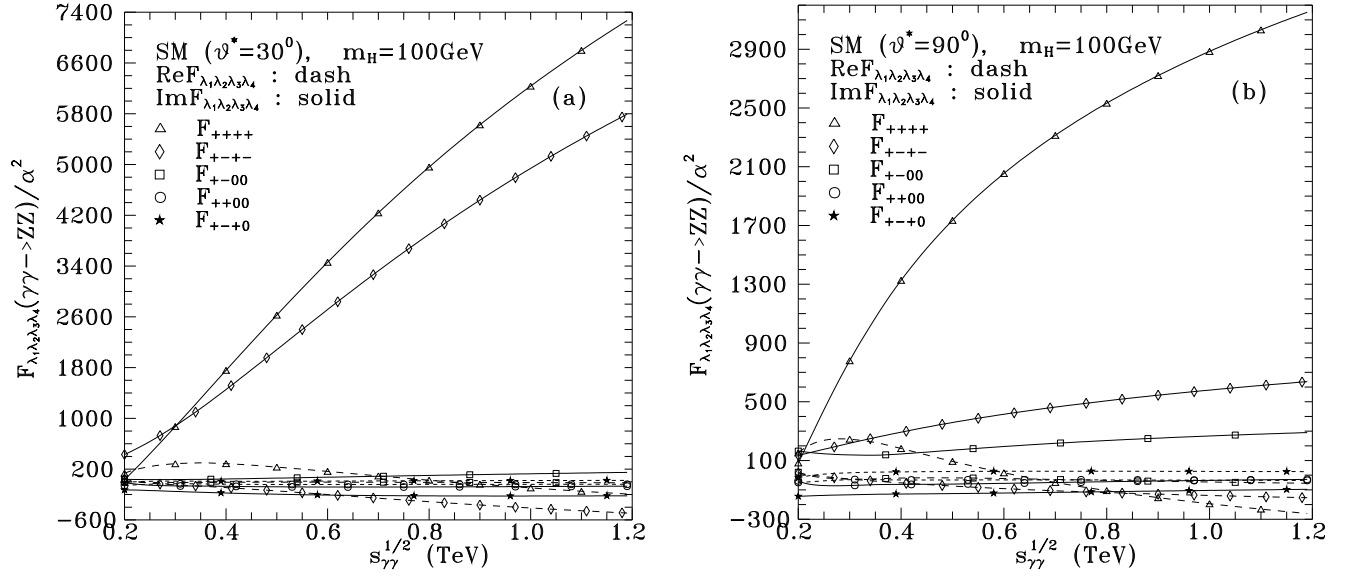


Figure 1: SM contribution to the dominant $\gamma\gamma \rightarrow ZZ$ helicity amplitudes at $\vartheta^* = 30^\circ$ and $\vartheta^* = 90^\circ$. All other amplitudes are predicted to be smaller or about equal to F_{+--+} .

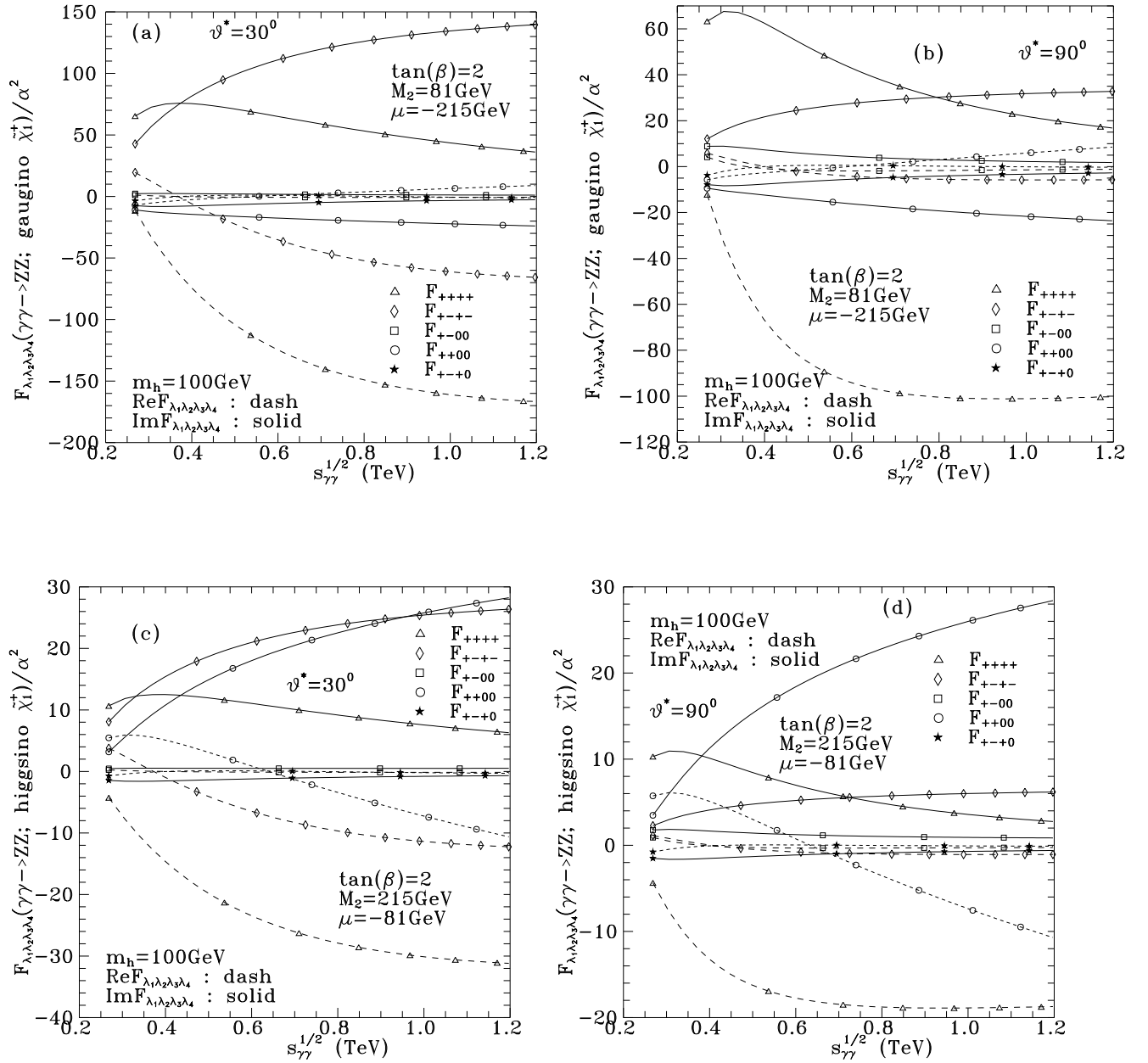


Figure 2: Chargino contribution to $\gamma\gamma \rightarrow ZZ$ helicity amplitudes for the gaugino and higgsino cases at $\vartheta^* = 30^\circ$ and $\vartheta^* = 90^\circ$. The parameters used are indicated in the figures and $Q_{\chi_1^+} = 1$.

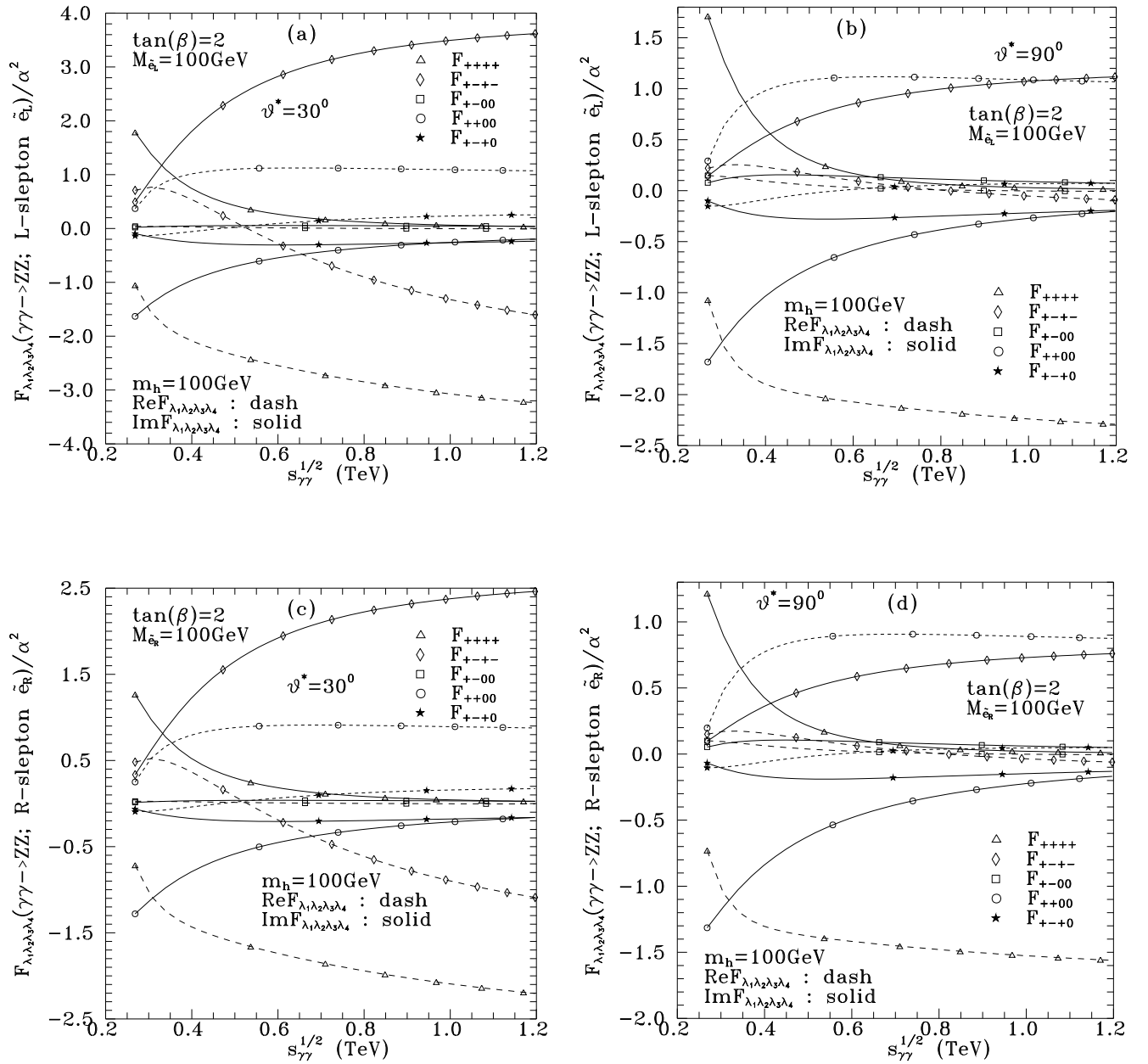


Figure 3: Contribution to $\gamma\gamma \rightarrow ZZ$ helicity amplitudes from a \tilde{e}_L^- or \tilde{e}_R^- loop, at $\vartheta^* = 30^\circ$ and $\vartheta^* = 90^\circ$. The parameters used are indicated in the figures and the slepton mass is taken $M_{\tilde{e}} = 100\text{GeV}$.

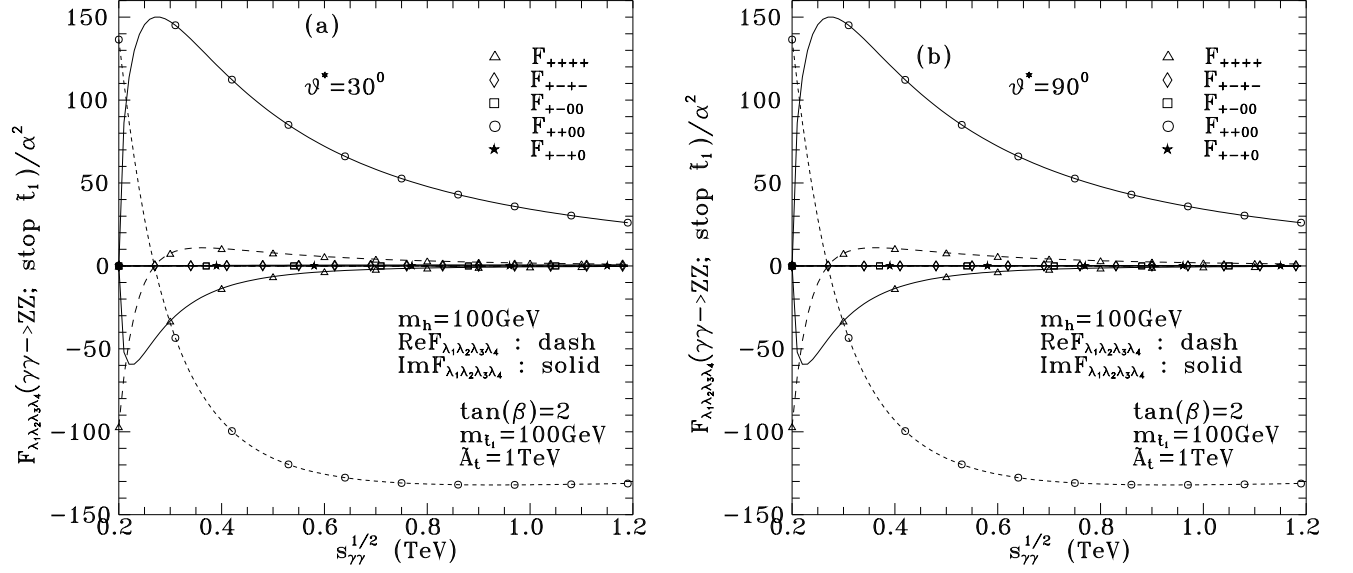


Figure 4: Contribution to $\gamma\gamma \rightarrow ZZ$ helicity amplitudes from the lightest stop \tilde{t}_1 at $\vartheta^* = 30^\circ$ and $\vartheta^* = 90^\circ$. The parameters used are indicated in the figures.

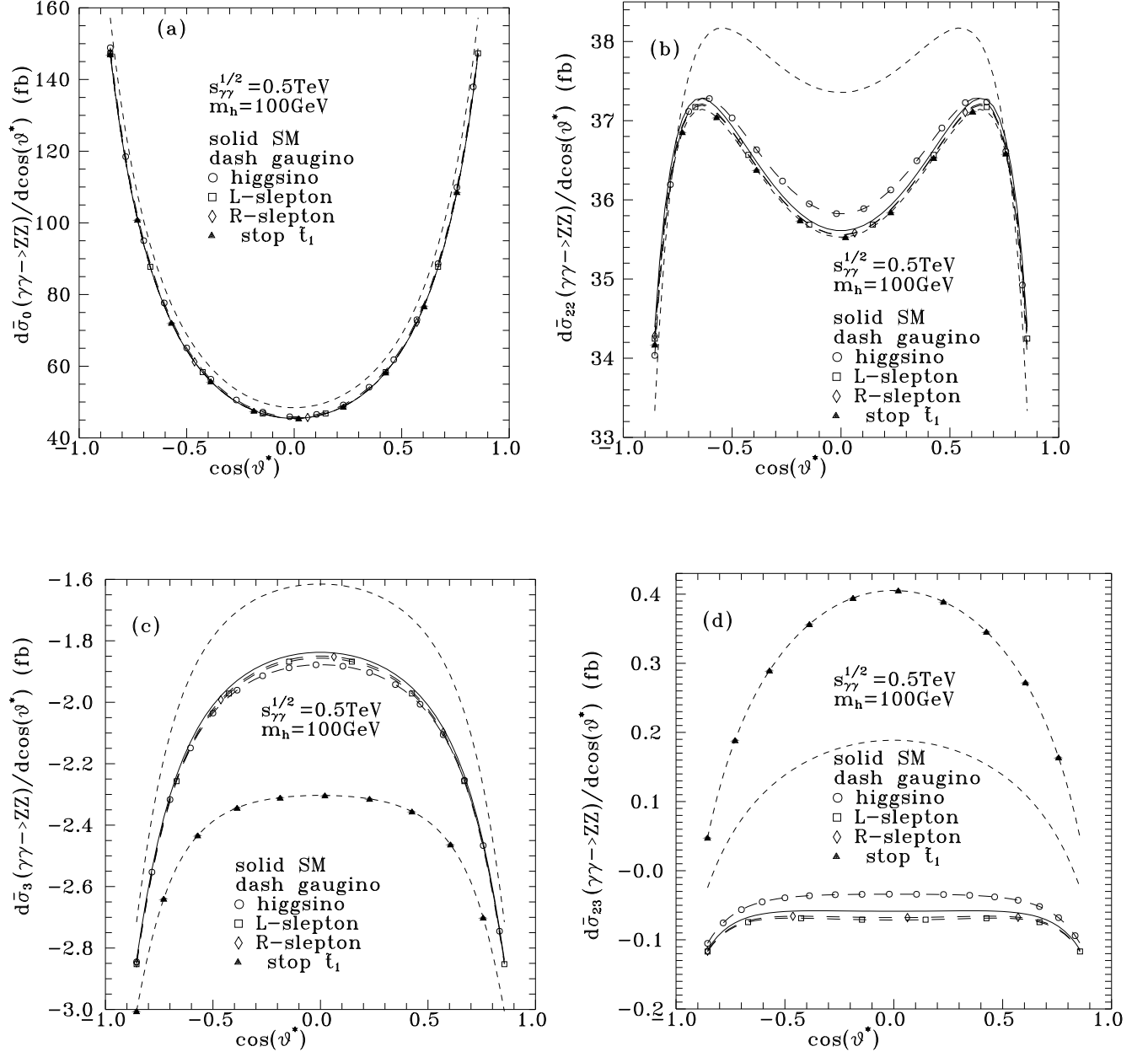


Figure 5: Angular distributions for $d\bar{\sigma}_0/d \cos \vartheta^*$, $d\bar{\sigma}_{22}/d \cos \vartheta^*$, $d\bar{\sigma}_3/d \cos \vartheta^*$, $d\bar{\sigma}_{23}/d \cos \vartheta^*$.

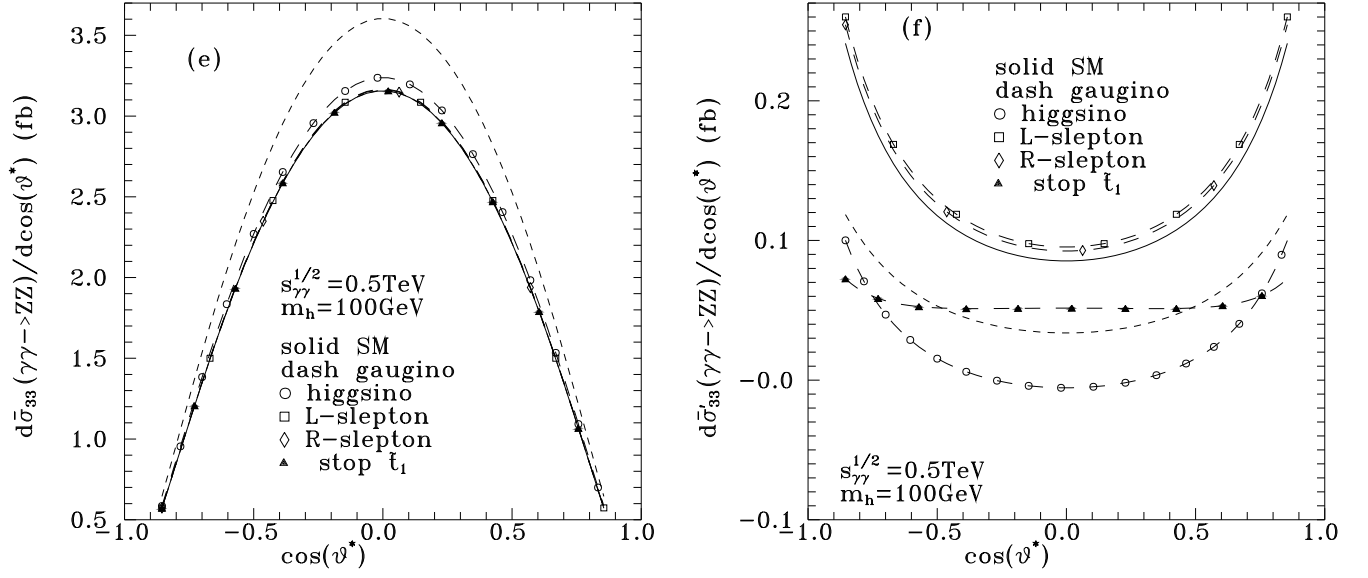


Figure 5: Angular distributions for $d\bar{\sigma}_{33}/d\cos\vartheta^*$, $d\bar{\sigma}'_{33}/d\cos\vartheta^*$.

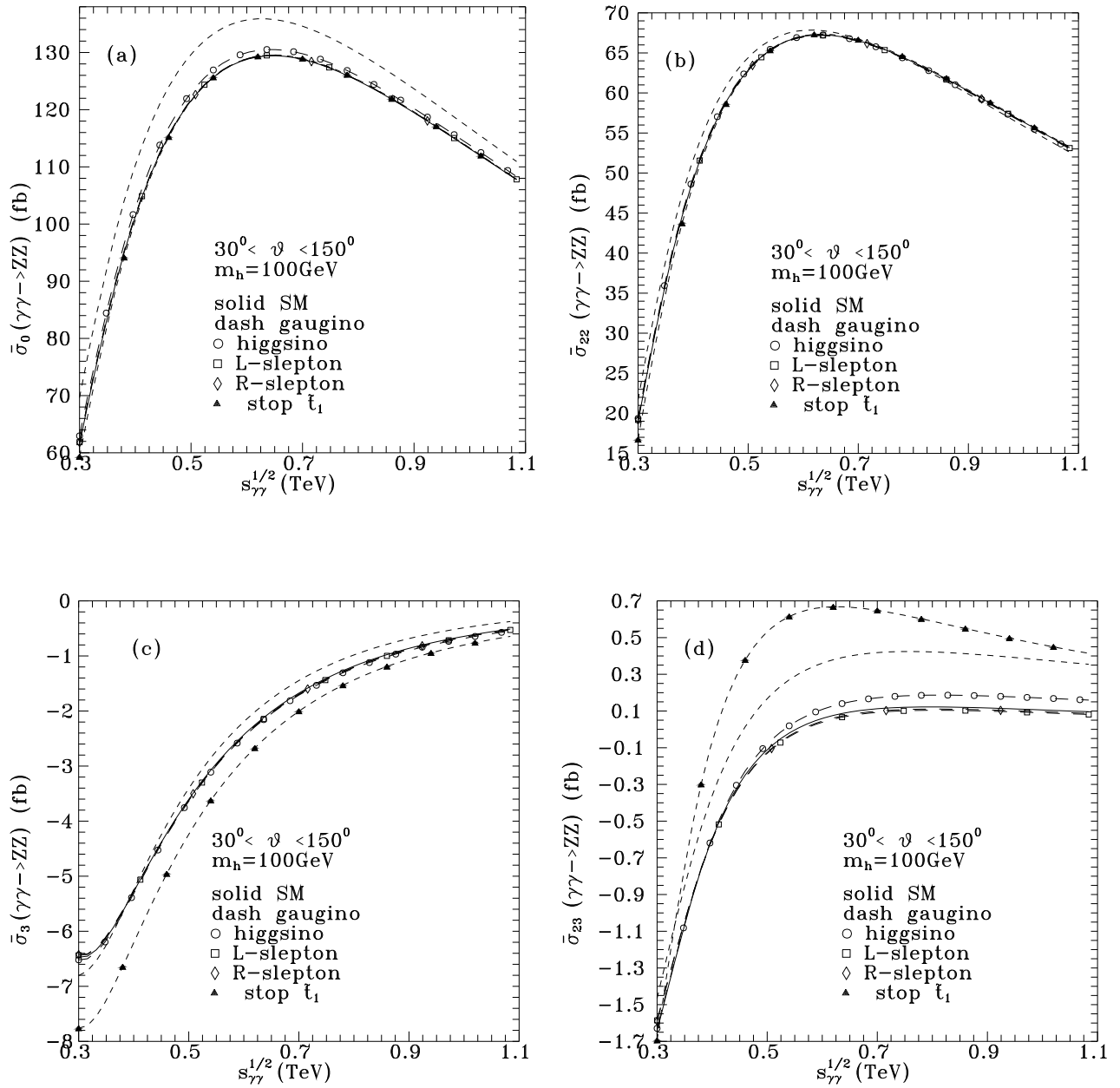


Figure 6: $\bar{\sigma}_0$, $\bar{\sigma}_{22}$, $\bar{\sigma}_3$ and $\bar{\sigma}_{23}$ for SM (solid) and in the presence of a chargino, or a selectron, or a lightest stop contribution, using the same parameters as in Fig.2 or Fig.3 or Fig.4 respectively.

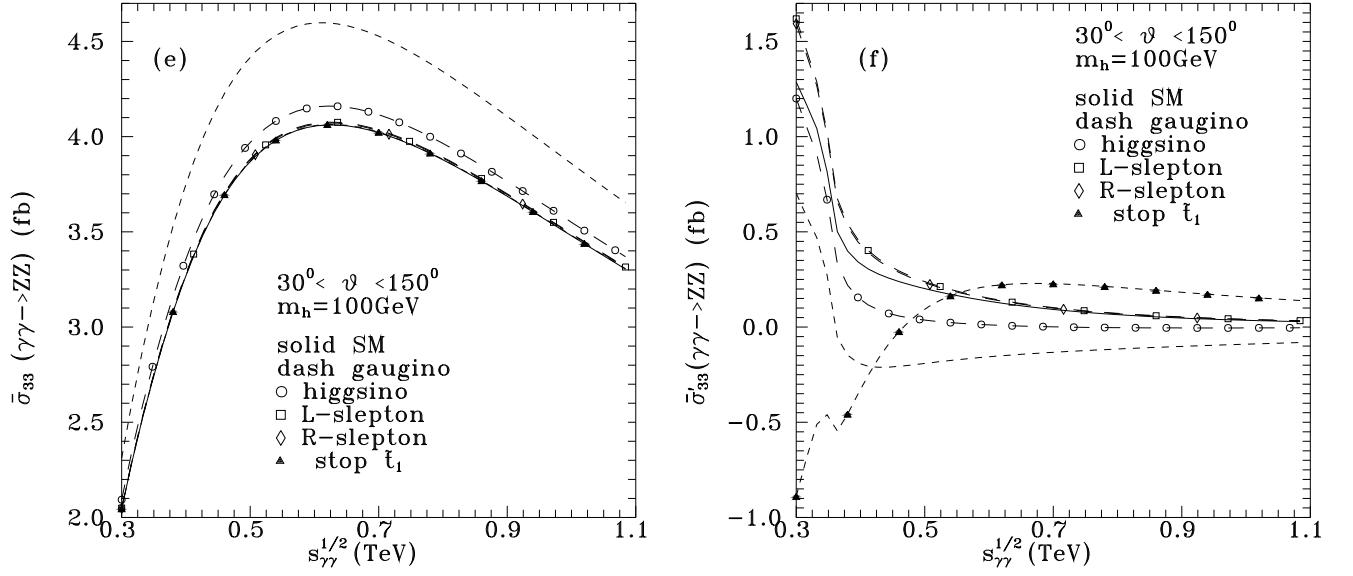


Figure 6: $\bar{\sigma}_{33}$ and $\bar{\sigma}'_{33}$ for SM (solid) and in the presence of a chargino or a selectron or a lightest stop contribution using the same parameters as in Fig.2 or Fig.3 or Fig.4 respectively.